UNIVERSITY OF CRETE – SCHOOL OF MEDICINE
Master of Science Degree
HEMATOLOGY-ONCOLOGY OF CHILDHOOD AND ADOLESCENCE

MASTER'S DISSERTATION

Molecular aspects of pediatric low-grade gliomas

TSAOULI GEORGIA

Pharmacist
PhD in Molecular Medicine

Heraklion, February 2021

Τριμελής Εξεταστική Επιτροπή
1. Ευτυχία Στειακάκη
2. Elisabetta Ferretti
3. Σοφία Αγγελάκη

This thesis is dedicated to my parents…

For their endless love, support and encouragement.

Table of Contents

Περίληψη

Μοριακά δεδομένα στα χαμηλού βαθμού κακοήθειας γλοιώματα της παιδικής ηλικίας

Τσαούλη Γεωργία

Τριμελής Εξεταστική Επιτροπή:
1. Ευτυχία Στειακάκη
2. Elisabetta Ferretti
3. Σοφία Αγγελάκη

Ημερομηνία: 25 Φεβρουαρίου 2021

Τα χαμηλού βαθμού κακοήθειας γλοιώματα της παιδικής ηλικίας (pLGGs) είναι μια ετερογενής ομάδα νευρογλοιακών όγκων βαθμού I και II, των οποίων η βασική θεραπευτική αγωγή είναι η χειρουργική εκτομή. Σε περιπτώσεις υποτροπής της νόσου, οι μετεγχειρητικές θεραπευτικές επιλογές περιλαμβάνουν κυρίως την χημειοθεραπεία ή/και ακτινοθεραπεία. Ωστόσο, αυτές οι δύο προσεγγίσεις μπορεί να μην οδηγήσουν στην θεραπεία του ασθενούς, ενώ ταυτόχρονα σχετίζονται με σημαντική μακροχρόνια τοξικότητα.

Το γονιδιωματικό τοπίο των pLGGs ακόμη διερευνάται και συνεχώς εξελίσσεται. Μέχρι σήμερα, έχει αναφερθεί η ενεργοποίηση της οδού PI3K/AKT σε αυτή τη νόσο, όμως οι μηχανισμοί ενεργοποίησής της δεν είναι ακόμη πλήρως κατανοητοί. Σε αυτή τη διπλωματική εργασία πραγματοποιήθηκαν πειράματα σε πρωτογενείς καλλιέργειες κυττάρων (τριών διαφορετικών ιστολογικών υποτύπων pLGGs), προκειμένου να μελετηθεί ο ρόλος του miR-139-5p στη σηματοδοτική πορεία PI3K/AKT στα υπερσκηνιδιακά γλοιώματα χαμηλού βαθμού κακοήθειας της παιδικής ηλικίας. Η υπερέκφραση του miR-139-5p σε αυτές τις καλλιέργειες ανέστειλε τον πολλαπλασιασμό των καρκινικών κυττάρων, μειώνοντας τα επίπεδα της φωσφορυλιωμένης AKT πρωτεΐνης και της φωσφορυλιωμένης p70-S6 κινάσης (p-p70 S6K). Πρωτείνες που εμπλέκονται στην ενεργοποίηση της οδού PI3K/AKT/mTORC1.

Παρά την πρόοδο στην εύρεση νέων μοριακών δεδομένων στα χαμηλού βαθμού κακοήθειας γλοιώματα της παιδικής ηλικίας, μέχρι σήμερα δεν υπάρχει κάποιος διαθέσιμος βιοδείκτης που να προβλέπει τη κλινική πορεία των ασθενών. Για το σκοπό αυτό, συλλέχθηκαν 104 δειγμάτα παιδιατρικών ασθενών από τέσσερα ευρωπαϊκά κέντρα νευρο-ογκολογίας και έγινε ανάλυση του προφίλ έκφρασης των microRNA τους. Η χαμηλή έκφραση των miR-376a-3p και miR-888-5p συσχετίστηκε με την εξέλιξη της νόσου και με δυσμενή συνολική επιβίωση. Τα επίπεδα έκφρασης αυτών των microRNAs, έπειτα από αναλύσεις εμπλουτισμού ομάδων γονιδίων για σηματοδοτικά μονοπάτια των miRNAs, συνδέθηκαν με την ανάπτυξη όγκων και την εισβολή των καρκινικών κυττάρων. Τα miR-376a-3p και miR-888-5p είναι ικανοί προγνωστικοί βιοδείκτες για την διαστρωμάτωση των ασθενών με χαμηλού βαθμού κακοήθειας γλοίωμα από τη στιγμή της χειρουργικής εκτομής.

Η εύρεση των παραπάνω μοριακών δεδομένων θα μπορούσε να συμβάλλει σημαντικά στην ανάπτυξη νέων εξατομικευμένων θεραπειών στα χαμηλού βαθμού κακοήθειας γλοιώματα της παιδικής ηλικίας.

Λέξεις κλειδιά: χαμηλού βαθμού κακοήθειας γλοιώματα, PI3K/AKT, βιοδείκτης, microRNA, δυσμενής κλινική πορεία, miR-139-5p, miR-376a-3p and miR-888-5p.

Abstract

Title: Molecular aspects of pediatric low-grade gliomas (pLGGs)

By: Tsaouli Georgia

Three Member Evaluating Committee:

1. Eftichia Stiakaki
2. Elisabetta Ferretti
3. Sofia Angelaki

Date: 25/2/2021

Pediatric low-grade gliomas (pLGGs) are a heterogeneous group of grade I and II glial tumors, whose mainstay of treatment is surgical resection. A subset of patients present tumor progression requiring adjuvant chemotherapy and/or radiotherapy, that often carry unsatisfactory results and long-term morbidity.

Several studies have focused and clarified the genomic aspects of pLGGs. To date, activation of the PI3K/AKT pathway in pLGGs has been reported, although activation mechanisms have not been fully investigated yet. Initially, we performed experiments based on previously published data that demonstrate the role of miR-139-5p in regulating PI3K/AKT signaling in supratentorial pLGGs. MiR-139-5p overexpression inhibited pLGG cell proliferation and decreased the phosphorylation of PI3K target AKT and phosphorylated-p70 S6 kinase (p-p70 S6K), a hallmark of PI3K/AKT/mTORC1 signaling activation.

Despite the progress in pLGG molecular characterization, up to date no biomarker predicting clinical outcome is available. For this purpose, microRNA profiles of 104 pLGG samples were collected from four European pediatric neuro-oncology centers and their microRNA profiles were analyzed.

Low expression of miR-376a-3p and miR-888-5p was associated with tumor progression and poor overall survival. Expression levels of these microRNAs, according to enrichment analyses, were linked to tumor growth and cancer invasion pathways.

These microRNAs might represent prognostic biomarkers able to stratify pLGG patients at the time of diagnosis. Additionally, the molecular aspects of these microRNAs could be significant for the identification of new target therapies.

Key words: pLGGs, PI3K/AKT, biomarker, microRNA, recurrence, miR-139-5p, miR-376a-3p and miR-888-5p.

Abbreviations

AG	Angiocentric glioma
Ago2	Argonaute
CLL	chronic lymphocytic leukemia
CNR1	Cannabinoid receptor 1
CNS	Central Nervous System
DA	Diffuse astrocytoma
DIG/DIA	Ganglioglioma/ Astrocytoma infantile desmoplastic
DNET	Disembrioplastic Neuroepithelial Tumour
FFPE	formalin-fixed paraffin-embedded
GG	Ganglioglioma
GTR	gross total resection
H/E	Haematoxylin and Eosin
LGGs	Low-grade gliomas
LOH	loss of heterozygosity
MEK	MAP/ERK kinase
miRNAs or miR	MicroRNAs
mTOR	Mammalian target of rapamycin
OA	Oligoastrocytoma
OG	Oligodendroglioma
OIS	oncogene-induced senescence
oncomiRs	oncogenic miRNAs
PA	Pilocytic astrocytoma
PFA	paraformaldehyde
PFS	progression free survival
pHGG	pediatric high-grade gliomas
pLGGs	Pediatric low-grade gliomas
PMA	Astrocytoma Pilomixoid
PR	partial resection
pri-miRNA	primary microRNA transcript
PXA	Pleomorphic Xanthoastrocytoma
RISC	RNA-induced silencing complex
RISC	RNA-induced silencing complex
ROC	Receiver Operating Characteristic Curve
SEGA	Gigantocellular Subependimal Astrocytoma
STR	subtotal resection
TEA	triethanolammine
TLDA	TaqMan Low Density Array
TRBP	transactivation-responsive RNA-binding protein
WHO	World Health Organization

1. Introduction

1.1 Pediatric low-grade gliomas

The most commonly diagnosed brain tumors in children are low-grade gliomas (LGGs), representing over 30% of tumors affecting the Central Nervous System (CNS) [1]. Pediatric LGGs (pLGGs) include different entities, as defined by the recently revised World Health Organization (WHO) Classification of CNS Tumors, which is based on both histological and molecular features [2]. This classification identifies nine categories of CNS tumors, of which four include tumors of glial or glioneuronal origin:

- Diffuse astrocytic and oligodendroglial tumors
- Other astrocytic tumors
- Other gliomas
- Glioneuronal tumors

The tumors belonging to these categories are also subclassified on the basis of their genetic characteristics [2]. Furthermore, the WHO classification system categorizes these tumors starting from grade I (lowest grade) to grade IV (highest grade), based upon histopathologic characteristics such as:

• similarity with normal cells (atypia);
• growth rate (mitotic index);
• growth rate and death of tumor cells in the neoplastic focus (necrosis);
• potential diffusion rate (widespread or focal);
• blood flow (vascularization)

Low-grade gliomas (LGGs) consist of grade I tumors, which contain none of the mentioned histologic features, and grade II tumors, characterized by the presence of cytologic atypia alone [2], and are classified in:

Table 1. Classification of diffuse gliomas.

Diffuse gliomas	WHO grade	Histological features (Pathological Anatomy)	Localization (Clinical Diagnosis)
Diffuse Astrocytoma (DA)	II	Irregular nucleus and hyperchromia; low mitotic index and absence of vascular proliferation.	Brain hemispheres. In pediatric age it can also arise in the brain stem or in the spinal cord.
Oligodendroglioma (OG)	II	Regular and uniform nucleus, clear cytoplasm, with a definite aspect to "honeycomb".	Bark and white matter of the brain hemispheres.
Oligoastrocytoma (OA)	II	Mixed characteristics between the two cell types.	Brain hemispheres.

Table 2. Classification of astrocytic tumors.

Astrocytic tumors	WHO grade	Histological features (Pathological Anatomy)	Localization (Clinical Diagnosis)
Pilocytic astrocytoma (PA)	I	Biphasic architecture with compact areas and non-homogeneous areas. The former show "piloid" processes and often multiple Rosenthal fibers. The latter show eosinophilic granular bodies. Limited mitoses.	Generally in the cerebellum, optical pathways, III ventricle. Sometimes basal ganglia or cerebral hemispheres.
Astrocytoma Pilomixoid (PMA)	II	Fusiform cells associated with perivascular dispositions on a loose fibrillar and myxoid background lacking Rosenthal fibers.	At the level of the chiasmus.
Gigantocellular Subependimal Astrocytoma (SEGA)	I	High phenotypic variability, hyalinization of the blood vessel wall, lymphocyte infiltrates and calcification. Furthermore, mitotic activity can be observed.	It originates in the wall of the lateral ventricles, near the foramen of Monro.

Pleomorphic Xanthoastrocytoma (PXA)	II	Large, pleomorphic tumor cells; often they have many eosinophilic and aggregated granular bodies of lymphocytes.	Predominantly in the cerebral hemispheres.

Table 3. Classification of other gliomas.

Other gliomas	**WHO grade**	**Histological features (Pathological Anatomy)**	**Localization (Clinical Diagnosis)**
Angiocentric glioma (AG)	I	Tumour characterized by monomorphic, bipolar or less frequently epithelial cells with parallel or radial orientation to the vessel walls.	Brain hemispheres.
Astroblastoma	I	Tumour cells with large cytoplasm, radially oriented around blood vessels with extensive processes.	Brain hemispheres.

Table 4. Classification of glioneuronal tumors.

Glioneuronal tumor	**WHO grade**	**Histological features (Pathological Anatomy)**	**Localization (Clinical Diagnosis)**
Ganglioglioma (GG)	I	Cancer ganglion cells generally have dysmorphic features and abnormal orientation. They often have granular eosinophilic bodies.	Temporal lobe.
Ganglioglioma/Astrocytoma infantile desmoplastic (DIG/DIA)	I	Characterized by the presence of a desmoplastic stroma rich in reticulina	Brain hemispheres
Disembrioplastic Neuroepithelial Tumor (DNET)	I	Specific glioneuronal component, represented by axonal extensions surrounded by oligodendrocytes immersed in patches of loose substance in which the neuronal bodies seem to "float".	The temporal lobe, the floor of the III ventricle and the hypothalamus.

The vast majority of pLGGs are pilocytic astrocytomas (PAs, Figure 1), and they are therefore the ones that have been studied most thoroughly. These tumors are driven by dysregulated signaling through the MAPK/ERK pathway, which leads to growth arrest referred to as oncogene-induced senescence (OIS) [3]. Less is known about the biological characteristics of less common pLGGs which include, among others, gangliogliomas (GGs), disembryoplastic neuroepithelial tumours (DNETs), and angiocentric gliomas (AGs).

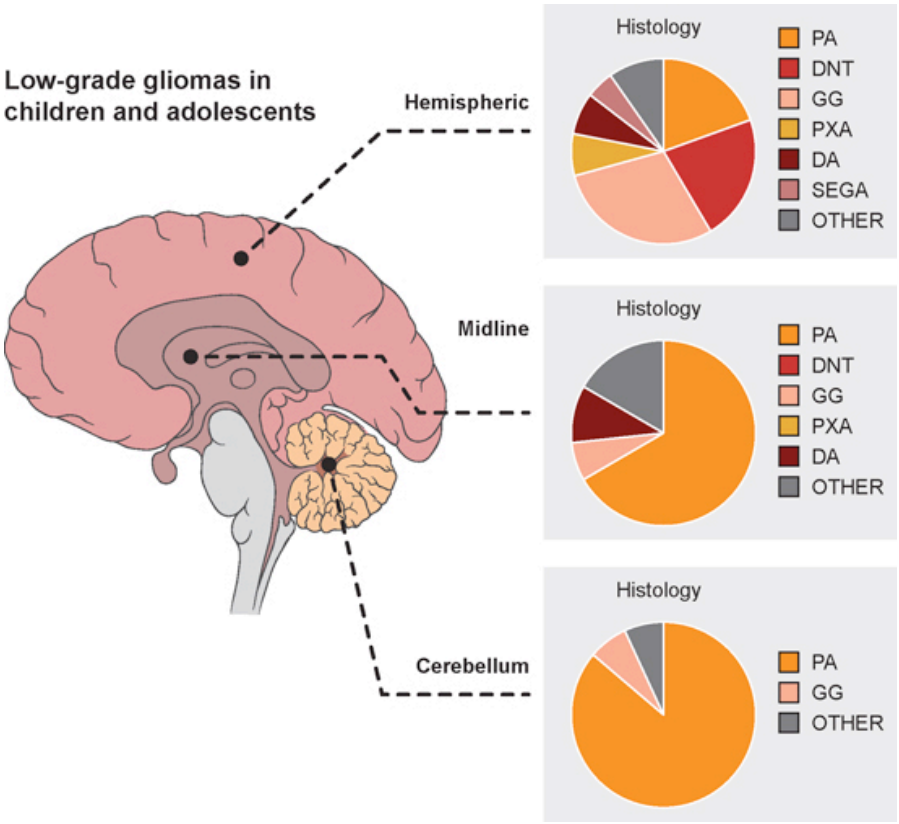

Figure 1. Low-grade gliomas in children and adolescents. *Distribution of histological subtypes of CNS tumours between adolescents and children [4].*

The genomic landscape of pLGGs is now being defined with accuracy by cytogenetic and genomic sequencing studies (Figure 2). Recent studies have stratified patients in different risk classes on the basis of selected genetic alterations [5] and on histological and clinical aspects [6]. The most frequent genetic alterations are the KIAA1549-BRAF fusion gene and the BRAF V600E single point mutation [7]. Other mutations, such as FGFR1 alterations (Figure 2), are mainly expressed only by specific pLGGs subtypes, such as DNET [8]. The BRAF gene is located on the long arm of chromosome 7q34 and encodes a protein involved in the MAPK signaling pathway, which plays a

crucial role in mediating a range of biological functions, including cell growth, survival, and differentiation.

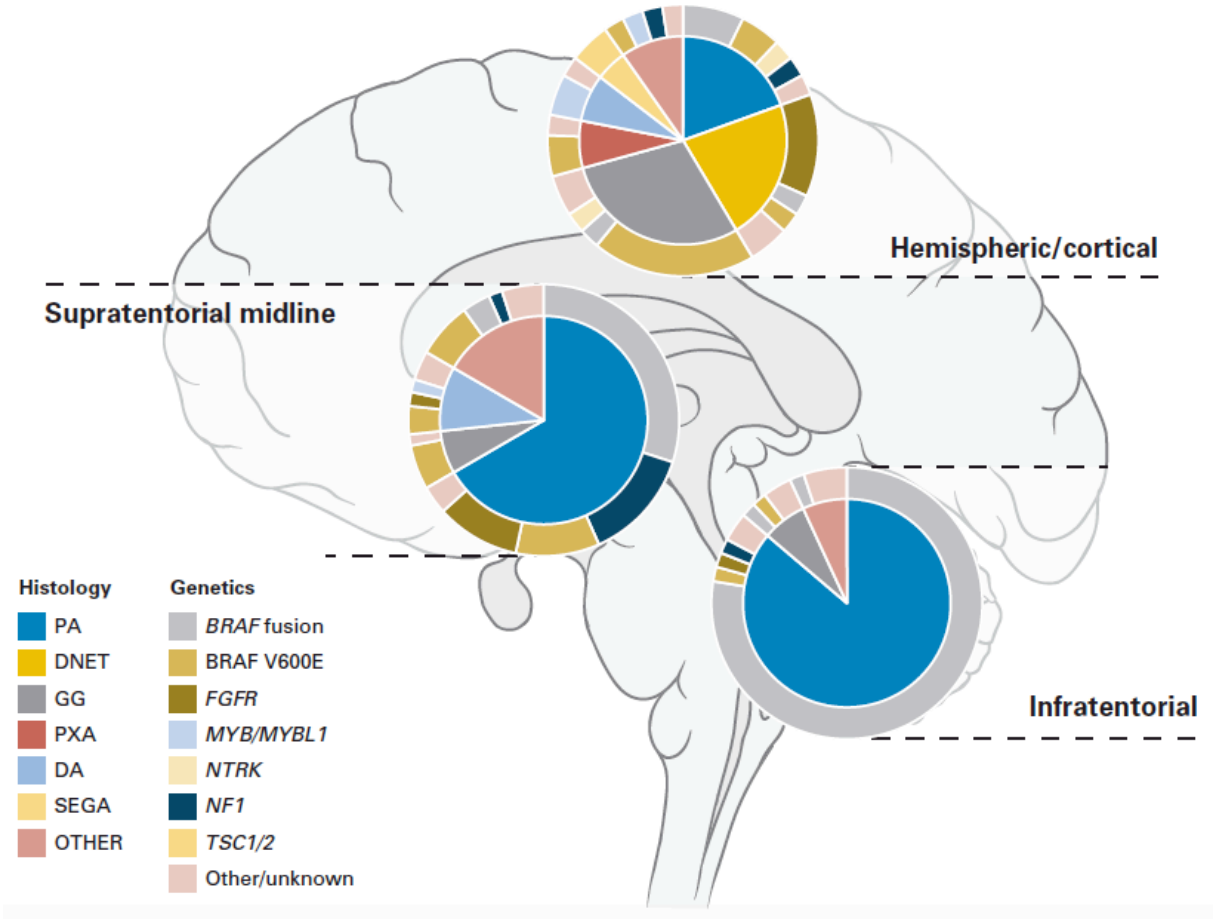

Figure 2. Distribution of histologies and molecular alterations of pLGGs on the basis of anatomical location. *The internal parts of the graphs represent the relative frequencies of the different pLGGs. The outer ring represents the most commonly found genetic alterations associated with each histological entity in the specific site of onset. DA, diffuse astrocytoma; DNET; neuroepithelial dysembryoplastic tumor; GG, ganglioglioma; PA, pilocytic astrocytoma; PXA, pilomixoid astrocytoma; SEGA, subependymal giant cell astrocytoma [9].*

The BRAF V600E point mutation consists of the replacement of a thymine with adenine at nucleotide 1796, with consequent amino acid substitution in the codon 600 of a valine with glutamate [10]. This mutation occurs at the level of the kinase domain, at the activation loop (A loop) or at the loop to which ATP (P loop) binds, causing a conformational change of the BRAF protein that becomes constitutively active. The highest frequency of the V600E mutation was found in PXAs (66%) and GGs (18%), while in PAs it represents 9% of cases [11]. As for the most common fusion of pLGGs, this occurs between BRAF and its centromeric gene, KIAA1549, following which transcription of different messengers is obtained after "alternative splicing". This in-frame fusion of KIAA1549-BRAF has been reported in 80% of sporadic PAs [12]. Most of these

KIAA1549-BRAF fusions occur between exon 16 of KIAA1549 and exon 9 of BRAF. However, there are at least six possible exon couplings for the KIAA1549-BRAF fusion (15: 9, 16:11, 16:10, 15:11, 17:10, 18:10) and in all the N-terminal of BRAF is replaced by that of KIAA1549. This results in a constitutive activation of the MAPK pathway, as the self-inhibiting N-terminal BRAF domain is lost while the C-terminal kinase domain is maintained [13,12].

The MAPK/Erk signaling cascade (Figure 3) is activated by a wide variety of receptors involved in growth and differentiation including receptor tyrosine kinases (RTKs), integrins, and ion channels. The specific components of the cascade vary greatly among different stimuli, but the architecture of the pathway usually includes a set of adaptors (Shc, GRB2, Crk, etc.) linking the receptor to a guanine nucleotide exchange factor (SOS, C3G, etc.) transducing the signal to small GTP-binding proteins (Ras, Rap1), which in turn activate the core unit of the cascade composed of a MAPKKK (Raf), a MAPKK (MEK1/2), and MAPK (Erk). An activated Erk dimer can regulate targets in the cytosol and also translocate to the nucleus where it phosphorylates a variety of transcription factors regulating gene expression [14]. Activated RAS is also capable of interacting with members of the phosphatidylinositol 3-kinase (PI3K) family. In particular, PI3K catalyzes the accumulation of PIP3, which promotes the recruitment of PDK1 at the membrane level, where it phosphorylates AKT, which in turn can phosphorylate a series of proteins that favor cell survival [15] (Figure 3).

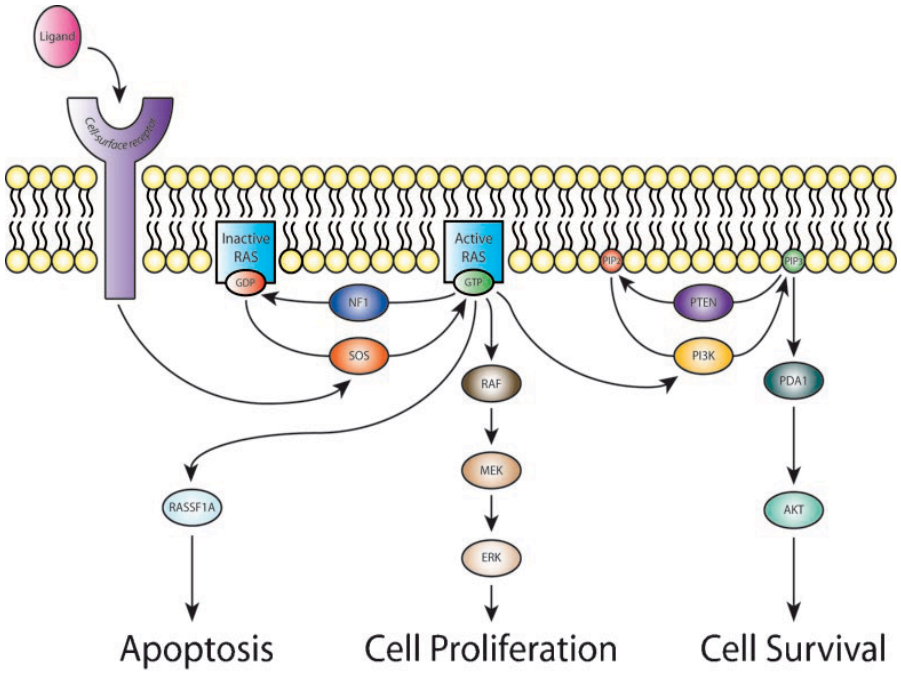

Figure 3. Schematic representation of the MAPK pathway. *The initiating event in MAPK pathway activation occurs when an extracellular ligand binds to one of several cell–surface receptors. The receptor-ligand complex activates an intracellular signaling cascade with the binding of RAS to GTP and its consequent activation. This process can be reversed by some GTPases, such as Neurofibromine 1 (NF-1), which catalyze the conversion of the active RAS-GTP form*

to the inactive RAS-GDP form. When RAS is activated it can interact with more than 20 different substrates, including members of the RAF family and PI3K [14]. This interaction allows the three RAF kinases (ARAF, BRAF and RAF1) to phosphorylate MEK1 and consequently activate ERK1 and ERK2. ERK proteins can phosphorylate different effector molecules with induction of cell proliferation [14]. PI3K instead catalyzes the transformation of the phosphorylation of phosphatidylinositol-4,5-bisphosphate (PIP2) and the subsequent production of phosphatidylinositol-3,4,5-trisfosfate (PIP3), a process inhibited by phosphatase homolog of the phosphatase and tensin (PTEN). The accumulation of PIP3 promotes the recruitment of PDK1 at the membrane level, where it phosphorylates AKT, which in turn can phosphorylate a series of proteins that favor cell survival [15].

One of the main mediators downstream of the PI3K/AKT pathway is the mammalian target of rapamycin (mTOR), in the form of 2 complexes: mTORC1 and mTORC2, as shown in Figure 4. Following its activation, the mTORC1 complex induces an increase in protein synthesis, stimulates cell growth and survival. The mTORC2 complex is less known, but appears to regulate metabolism, survival through AKT activation and cytoskeletal organization [16].

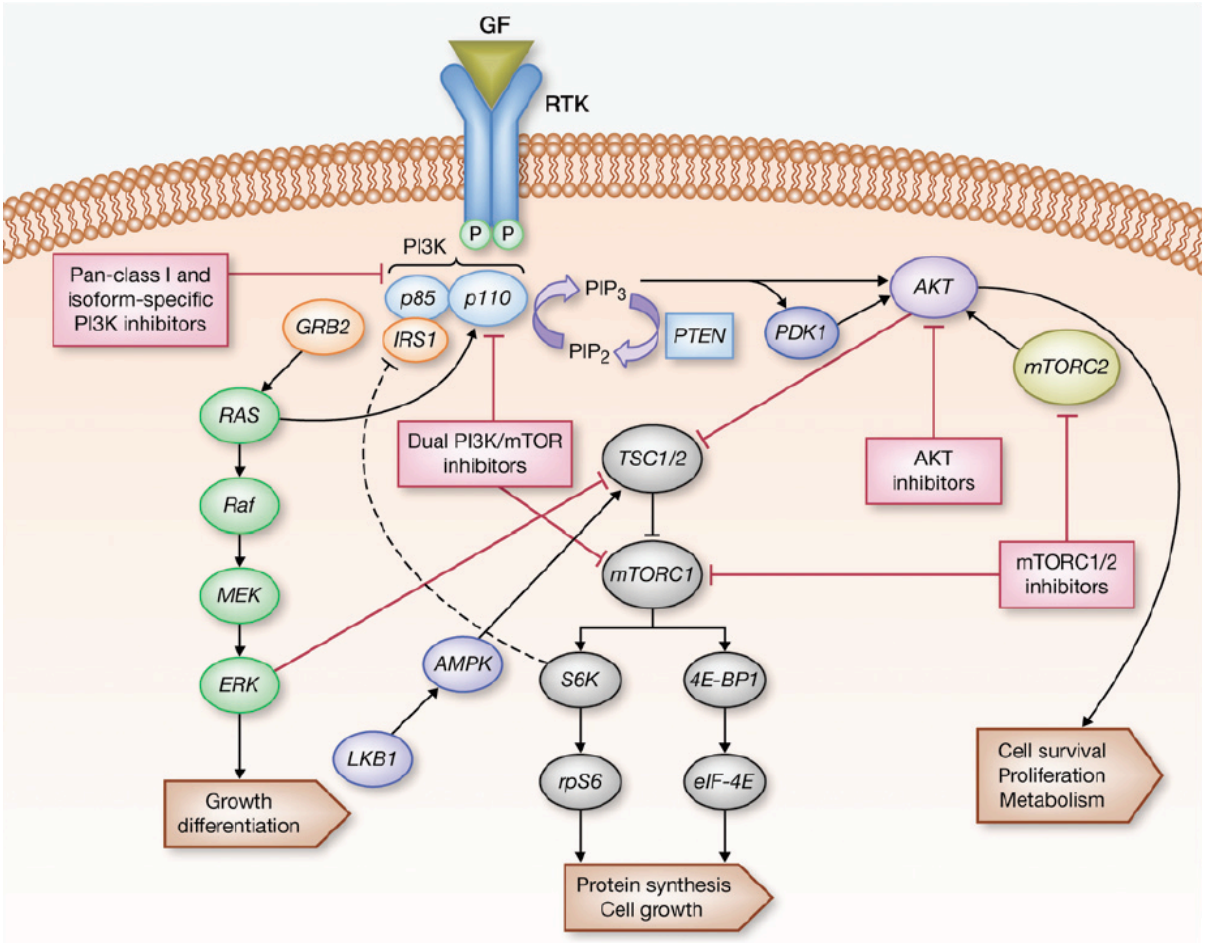

Figure 4. Overview of the PI3K/AKT/mTOR signaling pathway [17].

Along with the above-mentioned dysregulated MAPK/ERK signaling [18-20], aberrant activation of the PI3K/AKT signaling pathway is also a well-documented feature of gliomas, which has also been

described in pLGGs [7,21,16]. In some cases, its deregulation has been linked to genetic, such as *BRAF* fusions, *FGFR1* duplications and *MYB* rearrangements [9] , or epigenetic modifications, but in many cases the mechanism underlying PI3K/AKT pathway activation is still unknown.

1.2 Clinical characteristics of pLGGs and outcomes

The pLGGs' site of onset has a major impact on the patients' outcome since it determines the tumor's resectability. From a clinical point of view, children with low-grade gliomas, regardless of histology, have signs and symptoms related to the site of tumor onset. In particular, tumors arising in the anterior portion of hypothalamus or in the floor of the third ventricle can cause diencephalic syndrome, tumors arising in the hemispheric site often cause epilepsy [22], those located in the cerebellum are associated with dysmetria and ataxia and tumors found to the optic nerve cause visual problems up to the total loss of sight [23]. In addition, a significant number of symptoms are linked to increased intracranial pressure caused by ventricular obstruction, these symptoms include headache (particularly in the morning), nausea, vomiting and lethargy.

Not only the symptoms but also the clinical course is closely related to the site of onset, as it represents the main determinant of resectability. Infratentorial pLGGs, which occur mainly in the cerebellum, can often be treated by surgery with an excellent long-term prognosis [24]. Supratentorial tumors and those arising in the brainstem are more difficult to resect, and residual or recurrent disease is, therefore, a common event, occurring in about 30% of the cases. Of note, these patients receive adjuvant chemotherapy and, in selected cases, radiotherapy (e.g. SIOP-LGG 2004 protocol) [25] but both treatments are associated with substantial long-term toxicity, and these tumors frequently evolve into chronic disease with high morbidity [1,3,7,9,26]. The treatment option following surgery is chemotherapy with carboplatin/vincristine [27], which allows to obtain a three-year survival of 58% [28] despite the presence of important systemic complications and neurocognitive alterations [29]. Regarding radiotherapy, it appears that nearly half of irradiated low-grade gliomas in children have a reduction of at least 25%. Despite these potential benefits, the risks of using radiation therapy on the developing nervous system have been well documented: treatment of the optic/hypothalamic tract can result in endocrine dysfunction, cerebrovascular disease, secondary malignancy and neuro-cognitive deficits, particularly in young children. Even the most recent radiotherapy approaches, where a greater amount of healthy brain tissue remains unaffected, are used as rescue therapies [28] and infants and children under the age of 3 are subjected only to chemotherapy [30]. Thus, the cost of

survivorship is often high, since patients frequently present long-term sequaele, such as epilepsy, vision loss and impaired motor skills [31]. Moreover, a subset of pLGGs can transform in higher grade gliomas and metastasize [1].

For these reasons, it is necessary to identify new target therapies that can reduce morbidity in pLGGs. Activation of the MAPK signaling pathway is found in a high percentage of pLGGs, especially in PAs [7,32], while activation of the PI3K signaling pathway with downstream activation of mTOR has been associated with a more aggressive subgroup of pLGGs [33]. Therefore, therapies that act by inhibiting these signaling pathways are excellent candidates for the development of molecules with fewer toxic effects and less long-term morbidity. Several molecules that inhibit the MAPK signaling pathway are currently used in several clinical trials on pLGGs. These drugs are subdivided into agents that inhibit MAP/ERK kinase (MEK) or directly BRAF [28]. However, first generation BRAF inhibitors, such as dabrafenib and vemurafenib, should not be used on patients expressing the KIAA1549: BRAF fusion gene as these agents have been shown to induce paradoxical activation of the MAPK signaling pathway leading to development of the tumor [29]. However, this effect has not been observed with second-generation inhibitors, which inhibit MEK kinase and are still being studied in several clinical protocols. Among these, the most extensively studied is Selumetinib, which resulted in stabilization of the disease in 37% of patients suffering from recurrent pLGGs [34]. In addition to monotherapies, clinical trials are currently underway with combination therapies that act on the MAPK pathway as well as therapies that directly inhibit the PI3K/mTOR signaling pathway [28]. Furthermore, recent laboratory evidence suggests that combinatorial therapies with inhibiting agents both the MAPK signaling pathway and PI3K/mTOR could provide synergistic results [35].

1.3 MircoRNAs

MicroRNAs (miRNAs) are short (18–24 nucleotides), endogenous, single-stranded RNA molecules that regulate gene expression at post-transcriptional level, by binding to sequences complementary to 3 'UTR (3' untranslated region) of the target mRNA [36]. The microRNA processing pathway has long been viewed as linear and universal to all mammalian microRNAs. This canonical maturation includes the production of the primary microRNA transcript (pri-miRNA) by RNA polymerase II or III and cleavage of the pri-miRNA by the microprocessor complex Drosha–DGCR8 (Pasha) in the nucleus. The resulting precursor hairpin, the pre-miRNA, is exported from the nucleus by Exportin-5–Ran-GTP. In the cytoplasm, the RNase Dicer in complex with the double-

stranded RNA-binding protein TRBP cleaves the pre-miRNA hairpin to its mature length. The functional strand of the mature microRNA is loaded together with Argonaute (Ago2) proteins into the RNA-induced silencing complex (RISC), where it guides RISC to silence target mRNAs through mRNA cleavage, translational repression or deadenylation, whereas the passenger strand is degraded, Figure 5 [37]. MicroRNAs and their targets constitute remarkably complex regulatory networks as a single microRNA can bind and regulate many different mRNAs and, conversely, different microRNAs can cooperatively bind to and control a single target mRNA [38].

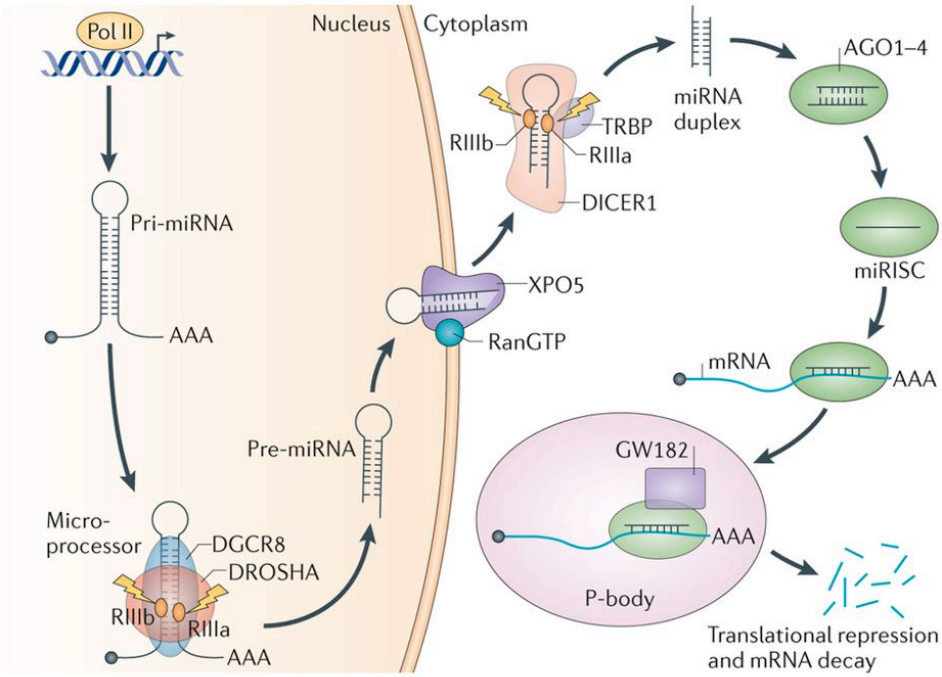

Figure 5. ***Biogenesis of miRNAs*** *[37].*

Many cellular pathways are affected by the regulatory function of microRNAs; the most prominent of these pathways control developmental and oncogenic processes. The first evidence of the involvement of microRNAs in human cancer derived from studies on chronic lymphocitic leukemia (CLL), particularly in an attempt to identify tumor suppressors at chromosome 13q14, frequently deleted in CLL. Dr. Croce's group reported that rather than along with containing a protein coding tumour suppressor gene, this critical region contains in fact two microRNA genes, miR-15a and miR-16-1, expressed in the same polycistronic RNA. This result provided the first evidence that microRNAs could be involved in the pathogenesis of human cancer as the deletion of chromosome 13q14 caused the loss of these two microRNAs [39].

Later, many groups of researchers identified the role of different microRNAs in human neoplasms, for example the amplification of the miR-17-92 cluster, strongly stimulated by c-Myc in B-cell

lymphomas and lung tumors, hinders the expression of tumor suppressors and therefore promotes cancer progression. During tumor development, microRNAs can be subject to "gain of function" mutations, when mutations cause an aberrant over-expression of microRNA, or "loss of function" if, on the other hand, the expression or normal function physiological microRNA fails. For this reason some microRNAs are identified as oncogenes or oncosuppressors, depending on how their expression varies in human neoplasms and their function in cellular processes linked to the gene targets they regulate [40]. The aberrant biogenesis of microRNAs in cancer can occur at different stages:

- At the transcriptional level, through specific transcription factors;
- Genetic alterations, such as amplification or loss of heterozygosity (LOH) affecting gene loci of microRNAs;
- Epigenetic modifications, for example methylation of CpG islands in tumour suppressor promoter regions.

1.4 MircoRNAs as biomarkers

MicroRNAs play an important role in various biological processes, such as cell development, differentiation, proliferation and apoptosis. The term "Biomarker" is used to indicate a biological, genetic and/or biochemical marker that can give diagnostic (e.g. concerning the probability of onset of a pathology) or prognostic indications (e.g. positive/negative response to a specific surgical and/or pharmacological intervention).

In oncology, an increased concentration of a biomarker can be indicative of disease status and any changes can be monitored in order to evaluate the effectiveness of specific therapeutic interventions.

A good biomarker is characterized by:

(a) a specific correlation with the disease;

(b) adequate prediction on the type of treatment and response;

(c) the possibility of carrying out the measurement easily, accurately and in a short time;

(d) being relatively insensitive to sampling errors.

MicroRNAs, due to their stability have been evaluated as promising and reliable biomarkers.

They are detectable in fresh frozen or formalin-fixed paraffin-embedded (FFPE) tissue [41,42], as well as in body fluids, such as blood, serum or plasma [43,44]. There are numerous important factors to consider in order to obtain a reliable analysis of microRNAs, such as: the quality of the sample, the extraction and detection method and sample storage.

In particular, it is essential to use a single extraction method, optimized and unformed, in order to minimize the variability and ensure the reliability of the results [45]. Numerous studies have performed microRNAs expression profiling by microarray and real time RT-PCR; more innovative techniques have recently been introduced such as sequencing platforms that have not only allowed to improve specificity and sensitivity but have also contributed to the discovery of new microRNAs [46]. These high throughput microRNA expression profiling studies have contributed in demonstrating the important role of microRNAs in carcinogenesis of different types of tumors [40,39,47-51]. Therefore, the differences found in microRNAs expression profiles between tumors and control samples (e.g. tissues from healthy donors) have revealed the possibility of using these molecules as promising diagnostic markers, often correlated with disease progression and patient survival. In this regard, it has been hypothesized that microRNAs may play a role as biomarkers in various pathologies, including CNS disorders [52].

1.5 MircoRNAs in pLGGs

The first microarray analysis of the expression profile of microRNAs in pLGGs was performed by the Birks group in 2011 in frozen tumor tissue samples. This analysis identified three microRNAs (miR-129, miR-142-5p and miR-25) differentially expressed in tumors compared to healthy controls [53]. In 2012, Ho et al. analyzed 43 PAs and from microarray analysis detected several downregulated microRNAs, including miR-124, miR-129, miR-138, miR-490, miR-7 and miR-873, and others upregulated, including miR-10b, miR-1260, miR-1274, miR-1288, miR-142, miR-143, miR-21, miR-92b, compared to controls [54]. Subsequently, Liu et al. analyzed the expression pattern of microRNAs from eight astrocytoma samples, divided according to malignancy. Through microarray and qRT-PCR they reported several upregulated microRNAs, such as miR-21, miR-181, miR-1321, miR-1259, miR-24, miR-222; and downregulated, such as miR-128, miR-885, miR-99b, miR-204, miR-218, miR-26a. In addition to the analysis of microRNAs, they also proceeded to investigate possible target genes and reported genes involved in the MAPK, Wnt/β-catenin and migration promoting receptor (EphB2) signaling pathway [55]. Later, Eguía et al. evaluated microRNA expression levels in 57 PAs samples of Mexican children, which included tumors from

grade I to grade IV. MiR-124-3p and miR-128-1 were downregulated in all astrocytomas compared to healthy brain tissues and this reduction was much more evident in grade IV astrocytomas. Furthermore, miR-128-1 levels were higher in infratentorial tumors than in supratentorial cases and miR-221-3p expression was higher in tumors without relapses and surviving patients [56]. Jones et al. focused on the differential expression of microRNAs in a cohort of 57 pLGGs samples. In PAs, compared to controls, they found a significant upregulation of miR-542-5p, miR-542-3p, miR-503, mir-450, miR-224, miR-146a and miR-34a. Target enrichment analysis of these upregulated microRNAs revealed regulators of the MAPK signaling pathway, such as KRAS, MEK1 or ERK1. MiR-21 and miR-146a presented instead gene targets belonging to NF-KB signaling [57]. In 2016 Braoudaki et al. analyzed the expression profile of microRNAs in a DNET cohort. 120 differentially expressed microRNAs were identified between these tumors and healthy brain tissue and two of these microRNAs (miR-1909 * and miR-3138) have been proposed as biomarkers capable of distinguishing DNETs from healthy subjects [58]. MiR-487b, belonging to the 14q32.31 cluster, a developmentally regulated microRNA cluster, is involved in glioma pathogenesis [59,60] and is down-regulated in gliomas [61]. More recently, Bongaarts et al. demonstrated the role of two microRNAs (miR-519d and miR-4758) in the regulation of the intracellular PI3K/AKT/p21 signaling pathway in pLGG associated with epilepsy, which include GGs and DNETs, and proposed these two microRNAs as biomarkers able to distinguish GGs from DNETs [62]. In addition, miR-125b has been found under-expressed in pleomorphic xanthastrocytomas and gangliogliomas [63]. MicroRNA profiling has also shown specific signatures in sporadic and NF1-associated PAs [64] and a low expression of miR-10b-5p has been reported along with its potential role in glioma invasion in NF1 mutated PAs in comparison with NF1 mutated high-grade gliomas [65]. In another study, parallel sequencing for transcripts and microRNAs was performed in subependymal giant cell astrocytomas and miR-20a-5p was identified as a possible regulator of both the MAPK/ERK and mTORC1 pathways, reported as possible targets for Tuberous sclerosis complex patients treatment [66].

Few studies have reported microRNAs as possible biomarkers of disease. MiR-92b was down-regulated in pLGG respect to pediatric high-grade gliomas (pHGG) and was proposed as a biomarker of poor prognosis [67]. Low levels of miR-29b-3p together with high level of its target gene, cannabinoid receptor 1 (CNR1), were suggested to be predictive of residual disease progression [68]. Finally, Tantawy et al. described 7 microRNAs (miR-10a, miR-29a, miR-361-5p, miR-617, miR-92a, miR-527, miR-206) as independent indicators for chemotherapy response [69].

In this context, a cohort of supratentorial pLGG including PAs, GG, angiocentric gliomas, DNET and glioneuronal tumors was investigated and all of them were characterized by low expression of miR-139-5p. Of note, this deregulation contributes to tumor growth via the pro-tumoral PI3K/AKT signaling pathway [70].

The above-mentioned studies highlight the fact that microRNAs in pLGGs play an important role in the regulation of a great variety of genes and, consequently, of multiple signaling pathways. This can be exploited in the early detection of disease, risk assessment and innovative therapeutic strategies.

2. Aim of the study

Pediatric low grade gliomas (pLGGs) are the most frequent brain tumors and with heterogeneous clinical and histological aspects. About 40% of patients with pLGGs can be surgically treated by complete resection of the tumor. For tumors occurring at the supratentorial level, however, total surgical resection is difficult to obtain and, following partial tumor resection, patients often experience disease recurrence as well as suffering from important co-morbidities due to the late effects of treatment. In oncology, microRNAs have assumed considerable importance both as regulators of gene expression, acting as oncogenes and/or onco-suppressors, and as biomarkers of disease.

Thus, aim of this project was to analyze a series of pLGGs samples to determine their microRNA profile. Focusing the study on deregulated microRNAs in supratentorial pLGGs, which present the poorest clinical outcomes, in order to identify new molecular aspects by investigating their functional and prognostic role.

Firstly, experiments were performed to extent previously published data that demonstrated the involvement of miR-139-5p with the oncogenic pathway of PI3K/AKT/mTORC1 in pLGGs tumors. The addition of new samples strengthens the suggestion for the development of novel targeted biological therapies that can reduce morbidity related to chemo and/or radiotherapy treatment.

A further aim of this thesis was to analyze and evaluate the role of microRNAs as biomarkers in pLGGs. The identification of microRNAs as prognostic biomarkers was focused on supratentorial pLGGs, the patients with worse prognosis, for which a complete surgical resection is not possible.

3. Materials and methods

Unless otherwise stated, commercially available products were used according to the manufacturer's instructions/protocols.

3.1 Cell treatments

Synthetic miR-139-5p (miRIDIAN microRNA code: C-310568-07; Dharmacon, Cornaredo, Milan, Italy) or negative control (miRIDIAN microRNA negative control code: CN-001000-01; Dharmacon) were transfected into pLGG primary cells [71] at 20 nM using HiPerFect transfection reagent (Qiagen Inc., CA, USA) for 48h. MiR-139-5p overexpression was confirmed by single assay qRT-PCR. For pharmacological inhibition of PI3K, LY294002 was purchased from Sellekchem, dissolved in DMSO and stored until used in aliquots at -80°C as 50 mM stock solutions. LY294002 and controls (CTRL) (0.1% DMSO) were diluted in culture medium just before use. After 30 min of treatment with 50 μM LY294002, cells were shifted in normal culture medium for a recovery period of 48h. Cell growth was evaluated after 48h by trypan blue exclusion assay. Specifically, the number of cells that did not take up trypan blue (viable cells) was counted both after transfection of synthetic miR-139-5p or negative control. The number of cells that took up trypan blue (nonviable cells) was counted. Each sample was measured in triplicate and repeated at least three times.

3.2 Western Blotting

Western blotting analysis was performed according to standard procedures, as reported elsewhere [72]. Blots were incubated with primary antibodies: rabbit anti-phospho-Akt (Ser473), rabbit anti-Akt, rabbit anti-phospho-p70 S6 kinase (Thr389), rabbit anti-p70 S6 kinase (Cell Signaling Technology, Danvers, MA), and mouse anti-GAPDH (Abcam, Cambridge, UK). HRP-conjugated secondary antisera (Santa Cruz, Biotechnology) were added, and binding was visualized by enhanced chemiluminescence (Perkin Elmer, MA, USA). Images were acquired with the BioRad ChemiDoc MP Imaging System (BioRad, Hercules, CA). BioRad associated Image Lab Software was used to perform densitometric analysis. Values are expressed as fold changes relative to GAPDH, used as internal control.

3.3 Characteristics of pLGG cohorts

The study was performed on 104 tumor samples collected from four European pediatric neuro-oncology centers.

The first cohort (Cohort I) from one European Unit, the DKFZ German Research Center in Heidelberg, included 75 pLGGs and the second cohort (Cohort II) from three independent European institutions (Bambino Gesù Children's Hospital, Agostino Gemelli University Policlinic and Marseille Hospital) included 29 pLGGs, all underwent surgery between 2014 and 2017 and were followed up for at least three years.

According to the extent of surgical resection on MRI after one month from surgery, patients were subdivided in those with gross total resection (GTR), when all the tumor mass was removed; or those with any residual, which includes subtotal resection (STR), where an amount between 90% and 50% of the mass was removed and partial resection (PR), less than 50% of the tumor was removed. Patients with any residual tumor (STR and PR) were further subdivided in with or without recurrence according to disease progression, on the basis of MRI evaluation during the follow up and/or clinical worsening [23] All patients before surgery were naïve for chemo and/or radiotherapy.

FFPE samples of each of the pLGGs sample used in the study were sectioned (3µm) and stained with haematoxylin and eosin for histology. All tumor diagnoses were then confirmed by consensus decision of three experienced neuropathologists using the WHO classification criteria [2].

Ethical approval (Rif. 5866) was obtained in accordance with the Helsinki declaration of 1964 and its later amendments. Informed consent was obtained from the patients, parents or guardians before enrollment, according to our ethical committee guidelines. The study was approved by the ethical committees of the competent structures and the families of the patients signed the informed consent for participation in the study. RNA and DNA used for the analyses were extracted from tumor samples with pathologist-confirmed tumor cell contents of 80% or more. Non-neoplastic brain tissue was used as control, as in [70].

Features of Cohort I

Cohort I comprised of 75 PAs, 19 of which supratentorial and 56 infratentorial. Clinical and pathological features of this cohort are reported in Table 5.

49 patients underwent GTR, while the remaining 26 patients underwent STR. The mean age at diagnosis was 7.6, while the median 7 years old. Among the GTR patients, the majority of the tumors were infratentorial (n=40, 82% of the GTR patients). Most frequent location was the cerebellum (n=34, 85%), followed by brain stem (n=4, 10%) and the fourth ventricle (n=2, 5%). Only 9 (18%) GTR tumors were located supratentorially, specifically three in the thalamus (33%), four in the third ventricle (44%), one in the parietal lobe (11%) and one in the optic chiasm (11%). Among the GTR patients, only three cerebellar tumors, out of 75 (6%), presented recurrence with a PFS average time of 11 months.

The STR subgroup presented a more homogeneous distribution between infratentorial (n=16, 61%) and supratentorial (n=10, 39%) cases. The majority of the infratentorial STR tumors were located in the brainstem (n=8, 50%), five arose in the cerebellum (32%), two in the fourth ventricle (12%) and only one in the spine (6%). All the STR supratentorial tumors involved midline structures: six were located in the optic pathways (60%), two in the thalamus (20%) and two in the third ventricle (20%). In the STR subgroup, 5 patients (19%) showed recurrence with a mean progression free survival (PFS) of 9 months.

Table 5. Clinical-pathological features of Cohort I patients.

Sample code	Age (years)	Gender	Site of onset	Histology	Type of resection	Progression	Progression Free Survival (months)	Overall Survival (months)	Mutational status
ICGC_PA101	18	F	Md Infra	PA	STR	W/O	7	7	WT
ICGC_PA104	3	F	Md Supra	PA	STR	W/O	6	6	WT
ICGC_PA108	5	F	Md Infra	PA	STR	W/O	4	4	K16B9
ICGC_PA113	1	F	Md Infra	PA	STR	W/O	3	3	V600E
ICGC_PA118	7	F	Md Supra	PA	STR	na	NA	NA	Fusion
ICGC_PA134	7	M	Md Infra	PA	STR	W/O	6	6	NACC2:NTRK2 (Ex4:Ex13)
ICGC_PA143	17	F	Md Infra	PA	STR	W/O	5	5	NF1 p.R13912fs (germline); p.Q2245X (somatic)
ICGC_PA144	2	F	Md Supra	PA	STR	W/O	4	4	CLCN6:BRAF Ex2:Ex11); BRAF p.E451D
ICGC_PA147	12	M	Md Infra	PA	STR	W/O	5	5	K16B9
ICGC_PA14	5	F	Md Supra	PA	STR	W/O	23	23	K15B9
ICGC_PA158	5	F	Md Infra	PA	STR	W/O	3	3	V600E
ICGC_PA159	5	M	Md Supra	PA	STR	W/O	3	3	QKI:NTRK2 (Ex6:Ex16)
ICGC_PA165	5	M	Md Infra	PA	STR	W/O	3	3	K16B9
ICGC_PA41	15	F	Md Infra	PA	STR	na	NA	NA	FGFR1 p.K655I, p.K656E
ICGC_PA4	1	M	Md Supra	PA	STR	W/O	22	22	K16B9
ICGC_PA54	4	F	Md Supra	PA	STR	WITH	4	12	WT
ICGC_PA55	5	F	Md Infra	PA	STR	WITH	4	24	K16B9
ICGC_PA59	5	F	Md Infra	PA	STR	W/O	24	24	K15B9
ICGC_PA62	4	F	Md Infra	PA	STR	WITH	7	17	K15B9
ICGC_PA64	4	M	Md Infra	PA	STR	W/O	20	20	K16B9
ICGC_PA69	6	F	Md Supra	PA	STR	WITH	17	17	NF1 Large deletion (somatic); p.Q1174fs (somatic); FGFR1 p.N546K
ICGC_PA71	2	F	Md Supra	PA	STR	WITH	5	16	NF1 p.Q959X (germline); large deletion (somatic)
ICGC_PA84	9	M	Md Supra	PA	STR	W/O	10	10	FGFR1 p.K656E; PTPN11 p.E76A

ICGC_PA89	8	M	Md Infra	PA	STR	W/O	6	6	FGFR1 ITD Kinase Domain
ICGC_PA91	3	F	Md Infra	PA	STR	W/O	6	6	K16B9
ICGC_PA9	15	F	Md Infra	PA	STR	W/O	23	23	K15B9
ICGC_PA100	1	F	Md Infra	PA	GTR	W/O	11	11	K15B9
ICGC_PA102	15	M	Md Infra	PA	GTR	W/O	4	4	FAM131B:BRAF (Ex3:Ex9)
ICGC_PA103	7	M	Md Supra	PA	GTR	W/O	8	8	K16B9
ICGC_PA105	13	F	Md Infra	PA	GTR	W/O	4	4	K15B9
ICGC_PA106	4	M	Md Infra	PA	GTR	W/O	4	4	Fusion
ICGC_PA107	4	F	Md Supra	PA	GTR	W/O	8	8	K13B9
ICGC_PA109	5	F	Md Infra	PA	GTR	W/O	9	9	K16B9
ICGC_PA110	12	M	Md Infra	PA	GTR	W/O	3	3	K16B9
ICGC_PA112	14	M	Md Supra	PA	GTR	W/O	8	8	RNF130:BRAF (Ex3:Ex9)
ICGC_PA11	11	F	Md Infra	PA	GTR	W/O	21	21	K16B9
ICGC_PA135	3	M	Md Infra	PA	GTR	W/O	7	7	K16B9
ICGC_PA138	11	F	Md Infra	PA	GTR	W/O	4	4	K16B9
ICGC_PA140	10	F	Md Supra	PA	GTR	W/O	4	4	BRAF p.T599_insT
ICGC_PA145	7	F	Md Infra	PA	GTR	W/O	4	4	K16B9
ICGC_PA150	2	M	Md Infra	PA	GTR	W/O	5	5	K16B9
ICGC_PA157	11	F	Md Infra	PA	GTR	W/O	3	3	K16B9
ICGC_PA162	7	M	Md Infra	PA	GTR	W/O	3	3	K15B9
ICGC_PA164	8	F	Md Supra	PA	GTR	W/O	3	3	WT
ICGC_PA23	1	F	Md Infra	PA	GTR	W/O	26	26	WT
ICGC_PA24	2	M	Md Supra	PA	GTR	W/O	21	21	K16B9
ICGC_PA25	3	M	Md Infra	PA	GTR	W/O	24	24	K16B9
ICGC_PA42	3	M	Md Infra	PA	GTR	W/O	24	24	K16B9
ICGC_PA46	9	M	Md Supra	PA	GTR	W/O	12	12	K16B9
ICGC_PA52	6	F	Md Infra	PA	GTR	WITH	5	12	Fusion
ICGC_PA53	10	M	Md Infra	PA	GTR	W/O	15	15	K16B11
ICGC_PA56	9	M	Md Infra	PA	GTR	W/O	12	12	K16B9
ICGC_PA57	6	F	Md Infra	PA	GTR	WITH	8	14	K19B9
ICGC_PA58	13	M	Md Infra	PA	GTR	W/O	12	12	MKRN1:BRAF (Ex4:Ex11)

ICGC_PA63	17	F	Md Infra	PA	GTR	W/O	12	12	K16B11
ICGC_PA65	16	M	Md Supra	PA	GTR	W/O	10	10	BRAF p.R506_insVLR
ICGC_PA70	6	M	Md Infra	PA	GTR	W/O	12	12	K16B9
ICGC_PA73	9	M	Md Infra	PA	GTR	W/O	10	10	K16B9
ICGC_PA74	7	M	Md Infra	PA	GTR	W/O	12	12	K16B9
ICGC_PA75	14	M	Md Supra	PA	GTR	W/O	12	12	V600E
ICGC_PA79	6	M	Md Infra	PA	GTR	W/O	8	8	K16B11
ICGC_PA81	14	M	Md Infra	PA	GTR	W/O	10	10	K10B10
ICGC_PA83	8	F	Md Infra	PA	GTR	W/O	12	12	K16B9
ICGC_PA85	4	F	Md Infra	PA	GTR	W/O	7	7	K15B9
ICGC_PA86	11	M	Md Infra	PA	GTR	W/O	8	8	K15B9
ICGC_PA87	4	F	Md Infra	PA	GTR	W/O	10	10	K16B9
ICGC_PA88	6	F	Md Infra	PA	GTR	W/O	8	8	K15B9
ICGC_PA8	7	F	Md Infra	PA	GTR	W/O	18	18	BRAF Ex15+34bp of intron15:Ex10
ICGC_PA92	12	M	Md Infra	PA	GTR	W/O	4	4	FGFR1 p.N546K
ICGC_PA94	4	F	Md Infra	PA	GTR	WITH	14	14	K15B9
ICGC_PA95	7	F	Md Infra	PA	GTR	W/O	8	8	K19B9
ICGC_PA96	15	F	Md Infra	PA	GTR	W/O	7	7	RNF130:BRAF (Ex3:Ex9)
ICGC_PA97	8	F	Md Infra	PA	GTR	W/O	12	12	K16B9
ICGC_PA98	8	M	Md Infra	PA	GTR	W/O	12	12	WT
ICGC_PA99	9	M	Md Infra	PA	GTR	W/O	7	7	K16B9

Md=Midline, PA=Pylocytic Astrocytoma, STR=Subtotal resection, GTR=Gross total resection, WITH=With recurrence, W/O=Without recurrence

Features of Cohort II

Cohort II comprised of 29 supratentorial Grade I pLGGs. All clinical and pathological data are reported in Table 6. Cohort II included different histologies and 6 patients underwent STR while 23 patients underwent PR.

Mean age was 7.42 years, with a median of 6. The most frequent histology was PA (n=18, 62%), followed by GG (n=6, 21%), DNET (n=4, 14%) and AG (n=1, 3%). Fourteen PAs (78%) were located in midline structures: five in optic pathways, five in the third ventricle and three in the thalamus. Only four (22%) arose in hemispheric structures. DNET and AG were hemispheric. Four GG arose in

the temporal lobe, while two in midline structures, specifically one in the diencephalon and one in optic pathways. Twenty patients (67%) experienced tumor recurrence with a PFS average time of 3 years and tumors were equally distributed between hemispheric (n=10, STR n=5 and PR n=5) and midline (n=10, all PR) areas. Nine patients (33%) did not recur, with tumors mostly located in midline structures (6 out of 9, 67%).

Table 6. Clinical-pathological features of Cohort II patients.

Sample code	Age (years)	Gender	Site of onset	Histology	Type of resection	Progression	Progression Free Survival (years)	Overall Survival (years)	Mutational status of BRAF
FFPE_Gesi_22233	5	M	H Supra	DNET	STR	WITH	2	9	
OPBG13P	10	F	H Supra	DNET	PR	WITH	5,4	8	WT
FFPE_Gesi_16526	13	F	H Supra	GG	STR	WITH	7	8	V600E (?)
FFPE_Gesi_19683	12	F	H Supra	GG	STR	WITH	2	9	WT*
FFPE_Gesi_22457	9	M	H Supra	GG	PR	WITH	7	10	V600E (?)
FFPE_Gesi_11364	12	M	H Supra	GG	PR	WITH	5	10	WT*
FFPE_Gesi_25595	4	M	H Supra	PA	PR	WITH	1	?	WT*
FFPE_Gesi_11720	2	M	H Supra	PA	PR	WITH	2	?	WT*
FFPE_Gesi_8380	16	F	H Supra	PA	STR	WITH	2	12	WT*
FFPE_Gesi_21617	6	M	H Supra	PA	STR	WITH	5	13	WT*
256 13	3,6	M	Md Supra	PA	PR	WITH	0,58	7	K15B9
OPBG45C	7	F	Md Supra	GG	PR	WITH	4	7	WT
OPBG62P	3,7	M	Md Supra	GG	PR	WITH	0,5	5	WT
OPBG51S	6,8	F	Md Supra	PA	PR	WITH	0,66	5	K16B11
119637 FF	6	M	Md Supra	PA	PR	WITH	1,58	14	K16B9

179435 FF	6	M	Md Supra	PA	PR	WITH	4,25	17	K16B9
177408 FF	6	M	Md Supra	PA	PR	WITH	0,75	12	WT*
123965 FF	8	F	Md Supra	PA	PR	WITH	2,08	16	K15B9
89636 FF	2	F	Md Supra	PA	PR	WITH	9,33	25	WT*
117945 FF	0,91	M	Md Supra	PA	PR	WITH	1,83	17	WT
FFPE_Gessi_1651	13	M	H Supra	AG	STR	W/O	8	8	WT*
OPBG54M	8	F	H Supra	DNET	PR	W/O	5	5	WT
OPBG54M FFPE (OPBG74M)	5	F	H Supra	DNET	PR	W/O	3	3	WT*
OPBG94C	5,3	F	Md Supra	PA	PR	W/O	3	3	WT*
OPBG43D	3	M	Md Supra	PA	PR	W/O	6	6	K16B9
OPBG58SP	5	M	Md Supra	PA	PR	W/O	5	5	WT
172524 FF	14	M	Md Supra	PA	PR	W/O	12	12	WT*
45723 FF	16	F	Md Supra	PA	PR	W/O	17	17	V600E
75683 FF	7	M	Md Supra	PA	PR	W/O	16	16	WT*

H=Hemispheric, M=Midline, DNET=Dysembryoplastic Neuropepithelial Tumor, GG=Ganglioglioma, PA=Pylocytic Astrocytoma, AG=Angiocentric Glioma, STR=Subtotal, PR=Partial, WITH=With recurrence, W/O=Without recurrrence, CR=Complete remission, DoD=Dead of Disease, SD=Stable Disease, PR=Partial Remission, NA=Not performed, ND=Not detected. BRAF screening was limited to the V600E point mutation and three fusion genes [KIAA1549-BRAF exon 16-exon 9 (K16B9), KIAA1549-BRAF exon 16-exon 11 (K16B11), KIAA1549-BRAF exon 15-exon 9 (K15B9)]. WT*= Not screened for BRAF K15B9

3.4 Genomic landscape of samples

All Cohort I samples were subjected to whole genome sequencing and 68 of them to RNA sequencing [32] (Table 1). Cohort II samples were analyzed for the two most common genetic alterations found in these tumors – namely, the BRAF V600E point mutation (V600E) and the KIAA1549:BRAF fusion gene [including the three most frequent variants: KIAA1549-BRAF exon 16-exon 9 (K16B9), KIAA1549-BRAF exon 16-exon 11 (K16B11), and KIAA1549-BRAF exon 15-exon 9 (K15B9)].

BRAF fusion analysis. BRAF fusion analysis was performed on tumor cDNAs with the Applied Biosystems Viia7 real-time qPCR (RT-qPCR) System, as described by Tian et al. [73] and validated by PCR based Sanger sequencing through amplification with specific pairs of primers flanking the fusion point between the KIAA1549 (in exon 15 or 16) and BRAF (in exon 9 or 11) genes, as described by Jones et al. [13]. The purified PCR products were sequenced on an ABI 3130 XL DNA analyzer (Applied Biosystems) using the BigDye Terminator v1.1 cycle sequencing kit (Applied Biosystems) and the forward or reverse primer used to perform the PCR. The primer sequences were as follows: KIAA1549 exon 15: 5'-CGG AAA CAC CAG GTC AAC GG-3'; KIAA1549 exon 16: 5'-AAA CAG CAC CCC TTC CCA GG-3'; BRAF exon 9: 5'-CTC CAT CAC CAC GAA ATC CTT G-3'; BRAF exon 11: 5'-GTT CCA AAT GAT CCA GAT CCA TTC-3'.

BRAF V600E mutation. DNA was extracted from fresh frozen samples and patient-derived pLGG cell lines using the QIamp DNA mini kit (Qiagen Inc., Valencia, CA, USA). Quantity and quality were evaluated with a Nanodrop ND-1000 spectrophotometer (Thermo Scientific). RT-qPCR was performed, as described by Diniz et al. [74], using TaqMan probes (Life Technologies, Waltham, MA, USA): BRAF_476_mu, which detects T>A transversion at position c.1799, and the reference-gene probe BRAF_rf. Threshold cycle (Ct) values were analysed using Mutation Detector™ Software (Life Technologies). Genomic DNA extracted from BRAF V600E and BRAF wild-type colon cancer cell lines, kindly provided by Prof. Matilde Todaro (University of Palermo), were used as positive and negative controls, respectively.

3.5 MicroRNA profiles

For Cohort I microRNA sequencing was performed in the DKFZ German Research Center Heidelberg, as previously described [75]. For Cohort II, microRNA expression profiling was performed on fresh frozen (FF) tissues using TaqMan Low Density Array (TLDA) microfluidic cards (Human miR v3.0, Applied Biosystems), as described below.

3.5.1 RNA extraction of pLGG tissues

Trizol Reagent (Invitrogen, Thermo Scientific, CA, USA) was used to isolate total RNA from fresh-frozen pLGG tissue samples and patient-derived pLGG cell lines. To increase the RNA yield of the tissue samples, 250 μg glycogen (Invitrogen, Thermo Scientific, CA, USA) were added for each milliliter of Trizol. Total RNA quantity and quality were evaluated with a Nanodrop ND-100 spectrophotometer (Thermo Scientific). For each sample, total RNA was reverse-transcribed (500 ng to 1μg) using a high-capacity cDNA reverse transcription kit (Applied Biosystems, Thermo Scientific).

3.5.2 MicroRNA profiling and data analysis

MicroRNA expression profiling was performed on the pLGG tumors using RT-qPCR with TLDA microfluidic cards (Human miR v3.0, Applied Biosystems), which detect the 754 best characterized members of the human microRNA genome. Each reverse transcriptase reaction was performed with specific primers according to Applied Biosystems protocols, as described in Catanzaro G. et al, 2018 [70]. Statistical analysis was performed with StatMinerTM software, v. 5.0 (Integromics TM, Granada, Spain). MicroRNA expression levels were normalized using the global expression normalization method and the comparative threshold cycle method was used to calculate the relative microRNA expression. MicroRNAs with Ct values > 33 were excluded. Differential expression between groups was assessed with the Limma test, and p values < 0.05 were considered to be statistically significant. A single-assay qPCR for assessment of miR-139-5p expression (Code:002289) was carried out in triplicate using the TaqMan Individual microRNA assays (Applied Biosystems), as previously described [76]. Information regarding microRNA clusters was obtained from miRBase v.21 (http://www.mirbase.org/) [77].

3.5.2a MicroRNAs clustering analysis

Dendrograms and heat maps were generated with the use of R (http://www.r-project.org/) using differentially expressed microRNAs as input. The Bray-Curtis method and the average linkage were used in hclust to cluster the samples and heatmap.2 to generate the heat maps [78].

3.5.2b DIANA mirPath analysis

The microRNAs that were differentially expressed in pLGGs were loaded into the DIANA mirPath tool (http://snf-515788.vm.okeanos.grnet.gr/) [79] for microRNA pathway analysis. MicroRNAs that were significantly dysregulated in the tumors were then analyzed to identify their putative targets.

3.6 MicroRNAs in-situ hybridization (ISH)

ISH was performed on four cases without recurrence (1 AG, 1 DNET, 2 PAs) and three cases with recurrence (2 GGs, 1 PA) for miR-376a-3p and on three cases without recurrence (1 DNET, 2 PAs) and three cases with recurrence (2 GGs, 1 PA) for miR-888-5p. The neoplastic area was identified on a Haematoxylin and Eosin section (H/E). Then, FFPE sections were cut in RNAse-free environment at 5 µm thick and baked overnight (O/N) at 60°C. Slides were de-paraffinized with xylene and hydrated in ethanol-descending scale before permeabilization with 22,5µg/mL Proteinase K (Qiagen) for 10 min at 37°C. Slides were then washed in PBS and underwent a second fixation with 4% Paraformaldehyde (PFA, Merck-Millipore) for 3 min at room temperature (RT). After washes, slides were equilibrated with 0.13M 1-Methylimidazole pH 8 (Merck Millipore) buffer for 15 min at RT, followed by crosslinking with 0.16M N-(3-Dimethylaminopropyl)-N'-ethylcarbodiimide hydrochloride (EDC, Merck Millipore) in Methylimidazole buffer for 2h at RT and washed in TBS at 4°C before performing acetylation reaction with 0.1M triethanolammine (TEA, Merck Millipore) and 0.25% acetic anhydride for 25 min at RT. Slides were then pre-hybridized in pre-hybridization buffer (25% formamide and 0.2% Triton X100 in 2X SSC) for 30 min at RT, followed by hybridization with the microRNA probe of interest in 50% formamide, 250 µg/mL tRNA (Invitrogen), 200 µg/mL salmon sperm DNA (Invitrogen), 10% dextran sulfate. Double digoxigenin-labeled LNA-modified probes (Qiagen) corresponding to mature miR-376a-3p (sequence: AUCAUAGAGGAAAAUCCACGU) and miR-888-5p (sequence: UACUCAAAAAGCUGUCAGUCA) were used as follows: miR-376a-3p 40 nM was

incubated O/N at 4°C, while miR-888-5p 200 nM was incubated for 1h at 47°C. After post-hybridization washes, slides were incubated with 1:100 anti-digoxigenin-AP (Qiagen) in TN buffer (0.1M Tris-HCl pH 7.5 and 0.15M NaCl) with 1% of donkey serum for 2h at RT. After further washing, sections underwent a colorimetric reaction by incubation with nitro-blue tetrazolium chloride/5-bromo-4-chloro-3'-indolyphosphate p-toluidine (NBT/BCIP; Roche) and 2mM Levamisole (Dako) at RT or at 4°C ON. To stop the reaction, slides were washed twice with KTBT (Qiagen) buffer and twice with water. Nuclei were counterstained with Nuclear Fast Red (Qiagen) for 30 sec, dehydrated in ethanol-increasing scale and mounted with Eukitt Quik-hardening mounting medium (Sigma Aldrich). Slides were checked by light microscopy (Nikon Eclipse S0i microscope) and captured with Aperio scanner (Leica Biosystems) at 20X and 40X magnification. The experiment was performed at least in triplicate and quantification was done on at least 300 cells per group. The number of positive cells for each sample was evaluated with FIJI by using the Andy's algorithm, an automated digital analysis system [80]. Unpaired t-test was performed using GraphPad Prism version 6 (La Jolla, California, USA) and p values < 0,05 were considered statistically significant.

3.7 Statistical analysis

MicroRNA sequencing data of Cohort I were analyzed as described in [75]. Samples were classified based on the presence or absence of recurrence and differential expression analysis was performed using the R package DESeq2 [81]. Clustering and heat-maps were also generated in R using the heatmap function.

MicroRNA expression profiling data from Cohort II were processed with Statminer^{TM} software v 5.0 (Integromics TM) and differential expression analysis between pLGG samples with and without recurrence was performed, as previously described [70]. Briefly, microRNA expression was normalized using the global normalization and differential expression was evaluated using the Limma test. P values < 0.05 were considered as statistically significant.

Univariate analyses using the General Linear Model (GML) for miR-376a-3p and miR-888-5p were performed using IBM SPSS Statistics version 25 (Armonk, New York, USA), taking into consideration the Progression Free Survival (PFS) as a covariate and the other clinical features as fixed factors. Univariate analyses were performed to determine the significance of the patient survival and clinical features on the expression of the microRNAs, along with the ability to account for their variation. In detail, the Tests of Between-Subjects Effects, an analysis of variance,

determined the significance of a feature, whereas the Parameter Estimates summarized the effect of each factor. $P < 0.05$ was considered statistically significant.

Receiver operating characteristic (ROC) curves for the microRNAs of interest were generated using GraphPad Prism version 6 (La Jolla, California, USA).

MicroRNA target determination was performed for miR-376a-3p and miR-888-5p using Ingenuity Pathways Analysis (IPA) (Qiagen, Hilden, Germany). The genes that were common for both microRNAs were used as input for enrichment disease analysis in IPA and the top 30 categories and diseases, containing the highest number of genes involved, are reported. Genes of interest were further investigated using the gene query in IPA.

Data reported from cell treatments are the means ± SD of at least three independent experiments each performed in triplicate. Unpaired t-test and Paired t-test were performed wherever appropriate using GraphPad Prism Software version 6.0 (La Jolla, California, USA), P values < 0.05 were considered to be statistically significant.

4. Results

4.1 miR-139-5p regulates proliferation of supratentorial pLGGs by targeting the PI3K/AKT/mTORC1 signaling

4.1.1 Low levels of miR-139-5p in pLGGs regulate tumor-cell proliferation

Low levels of miR-139-5p in pLGGs were reported to regulate tumor-cell proliferation and further experiments were performed to strengthen these findings. MiR-139-5p levels in supratentorial pLGGs were markedly lower than those in non-neoplastic total brain tissues (Figure 6a). Downregulation of miR-139-5p was also evident in patient-derived primary pLGG cell cultures at levels comparable to those of the primary tumors they derive from (data not shown). Overexpression of miR-139-5p in these cells (Figure 6 b, c, d) resulted in significantly reduced proliferation, which was evident in all three histological types represented (Figure 7), while not affecting cell death (data not shown).

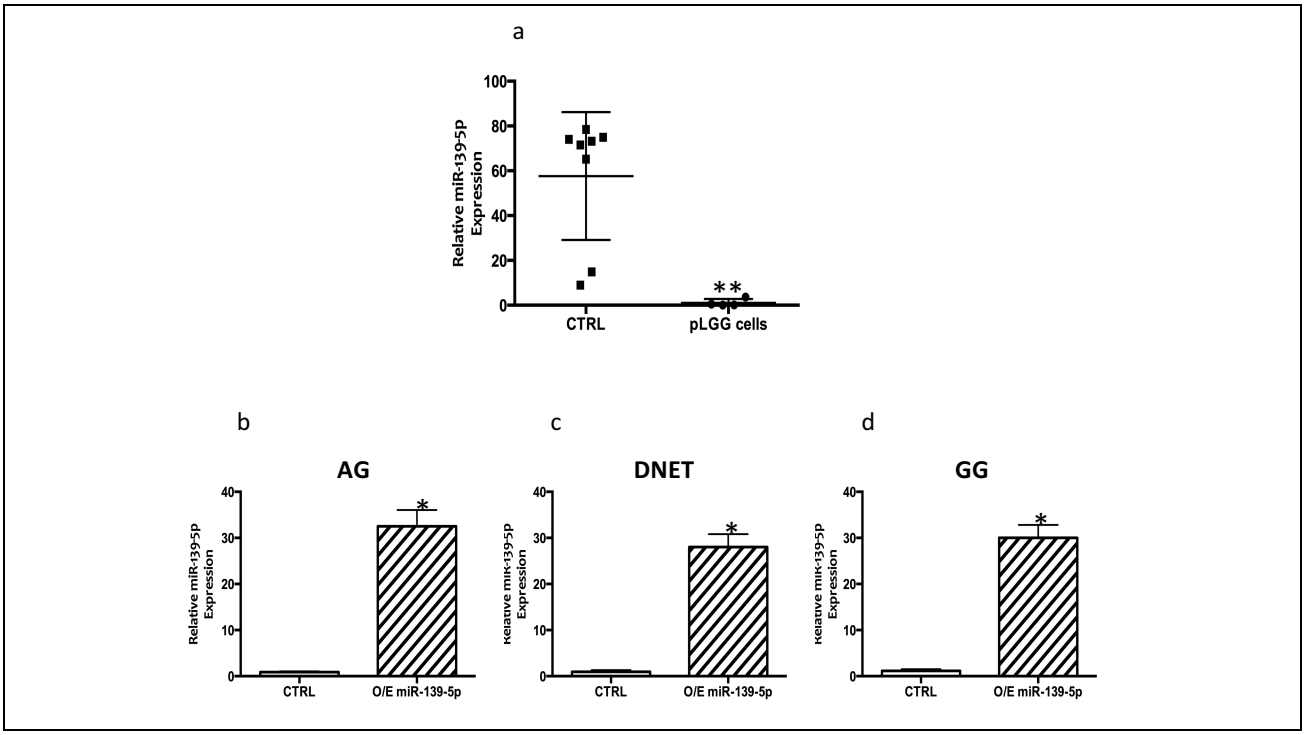

Figure 6. Levels of miR-139-5p before and after its overexpression in the four primary pLGG cell lines (derived from an AG, two DNETs, and a GG). *Cells were transfected with 20 nM miR-139-5p and assayed 48 h later. (a) MiR-139-5p level in non-neoplastic brain tissues (CTRL) was 68-fold higher than that found in the pLGG cells at baseline. (b-d) Post-transfection assays of (b) AG cells, (c) DNET cells, and (d) GG cells revealed mean miR-139-5p levels approximately 30-fold higher than those found at baseline (CTRL).* p<0.05, *** p<0.001 versus indicated CTRL.*

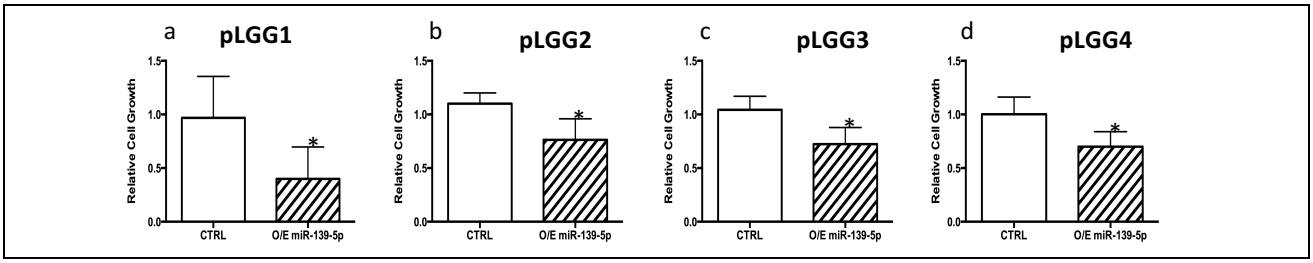

Figure 7. Effects on cell proliferation of miR-139-5p overexpression in cultured cells. *Relative cell growth of cultured cells from (a) primary AG indicated as pLGG1, (b) primary DNET indicated as pLGG2, (c) primary DNET indicated as pLGG3 and (d) primary GG indicated as pLGG4. Cells were transfected with 20 nM miR-139-5p or an empty vector (CTRL) and subjected to trypan blue staining 48 h later. Relative cell growth refers to fold over CTRL. * p<0.05 versus CTRL.*

4.1.2 miR-139-5p controls PI3K/AKT/mTORC1 signaling in supratentorial pLGGs

The results of the previous experiments provide evidence that downregulation of miR-139-5p plays a role in supratentorial pLGG cell growth. To determine whether its effects on cell growth were mediated by de-repressed PI3K activity, the effects of miR-139-5p overexpression were assessed on the phosphorylation of the PI3K target, AKT. At baseline, phosphorylated AKT (p-AKT) levels were high in all the cell cultures tested, but they dropped markedly after miR-139-5p overexpression, Figure 8.

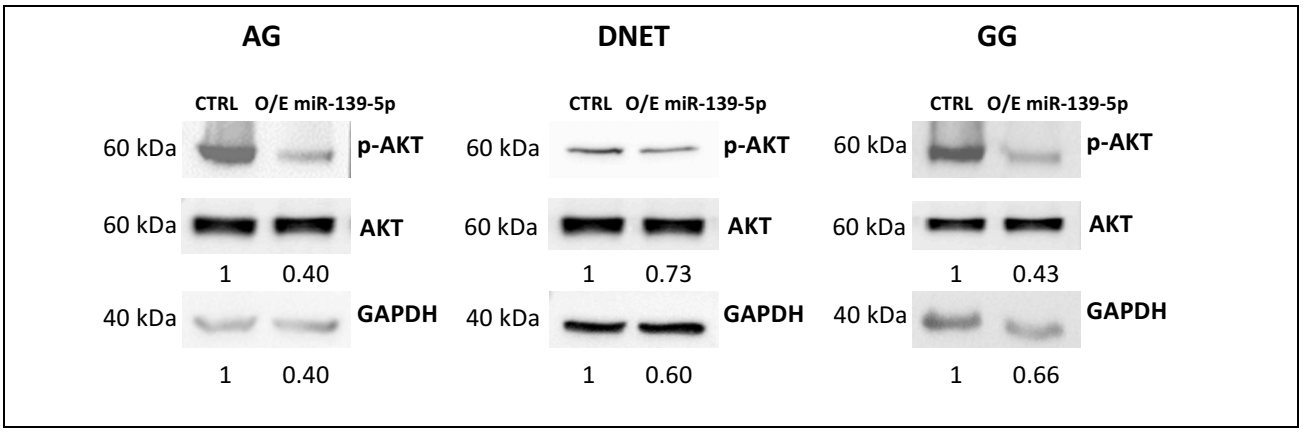

Figure 8. PI3K/AKT signaling pathway inhibition decreases pLGG AKT phosphorylation. *Phosphorylated AKT (p-AKT) levels were measured in supratentorial primary pLGG cells transfected with miR-139-5p or empty vector (CTRL).*

One of the downstream effectors of PI3K/AKT signaling is mammalian target of rapamycin complex 1 (mTORC1). Activation of this complex has already been reported in pLGGs [21], and hyper-activation of the PI3K/AKT/mTORC1 axis has been implicated in the increased cell

proliferation of these tumors [16]. The possibility that mTORC1 inhibition was involved in the anti-proliferative effects produced in pLGG cells by miR-139-5p overexpression was then investigated. As shown in Figure 9, cells transfected with miR-139-5p displayed significantly decreased phosphorylation of p70 S6K (p-p70 S6K), a hallmark of mTORC1 activation.

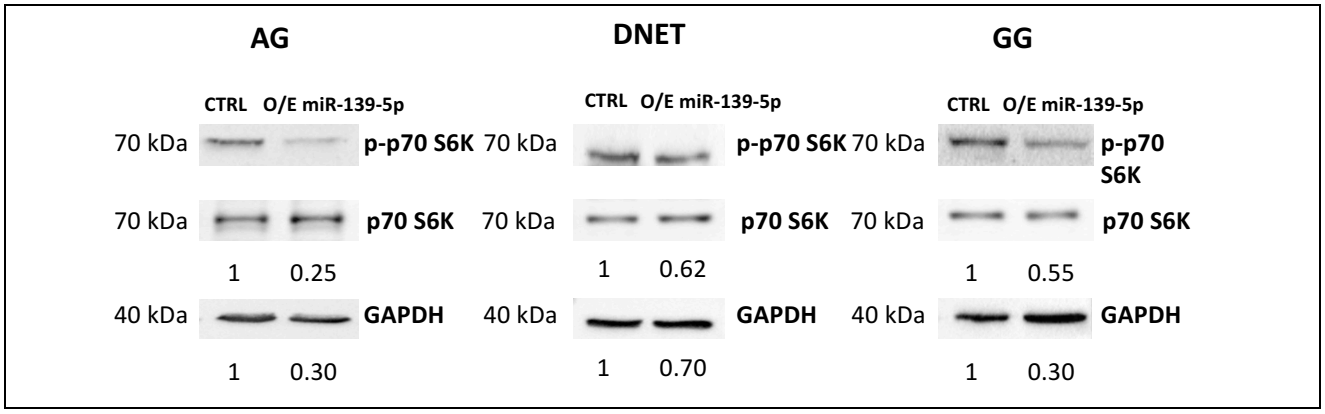

Figure 9. Phosphorylation of p70 S6K in pLGG cells subjected to miR-139-5p overexpression. *Phosphorylated p70 S6K (p-p70 S6K) levels were measured in supratentorial primary pLGG cells transfected with miR-139-5p or empty vector (CTRL).*

In order to confirm that miR-139-5p effect was directly mediated by PI3K inhibition, proliferation (Figure 10), p-AKT (Figure 11) and p70 S6K levels (Figure 12) in primary pLGG cells before and after treatment with the direct PI3K inhibitor LY294002 were examined. No significant effect on cell death was observed. A comparable reduction was produced when PI3K was inhibited with LY294002, cells transfected with miR-139-5p displayed significantly decreased phosphorylation of p-Akt and p70 S6K (p-p70 S6K).

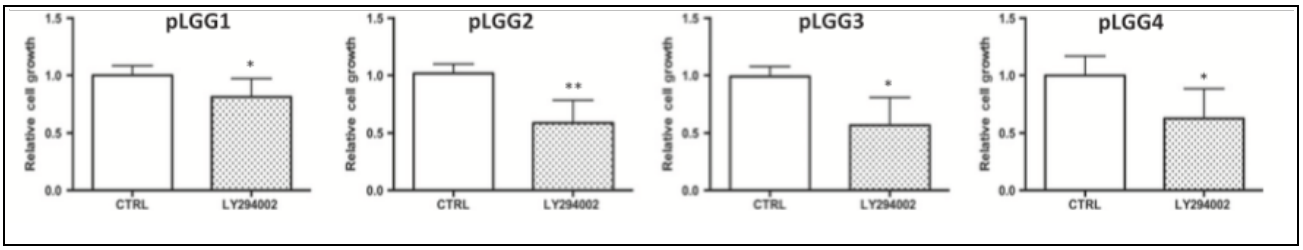

Figure 10. Effects on cell proliferation after 30 min treatment with 50μM LY294002 (assayed for proliferation by Trypan blue exclusion, after a 48h recovery period in normal medium). *Relative cell growth of cultured cells from (a) primary AG indicated as pLGG1, (b) primary DNET indicated as pLGG2, (c) primary DNET indicated as pLGG3 and (d) primary GG indicated as pLGG4. Relative cell growth refers to fold over CTRL. *P < 0.05, **P < 0.001 vs. CTRL. PLGG, pediatric low-grade gliomas.*

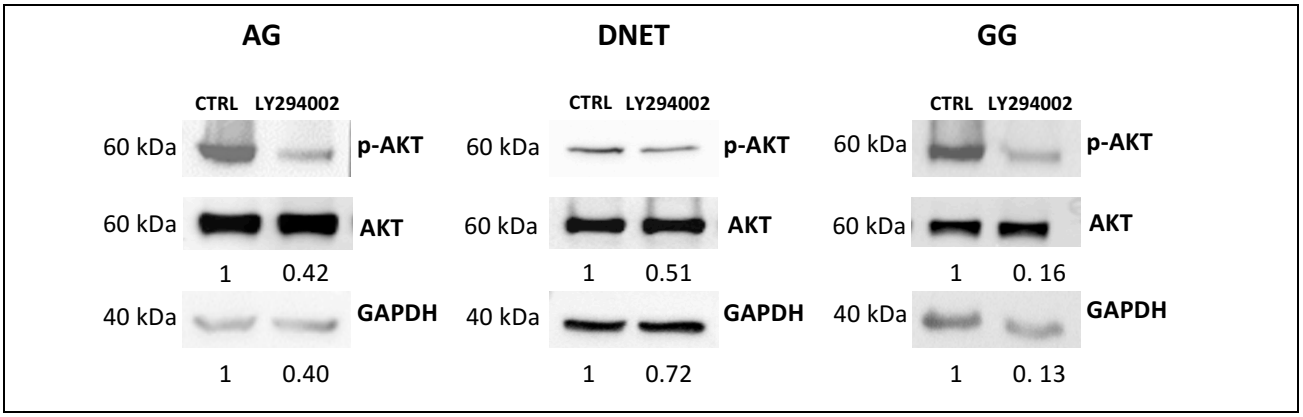

Figure 11. PI3K/AKT signaling pathway inhibition decreases pLGG AKT phosphorylation. *p-AKT and total AKT levels were measured in supratentorial primary pLGG cells treated with 50 μM LY294002 for 30 min or vehicle alone (CTRL) after a 48h recovery period in normal medium.*

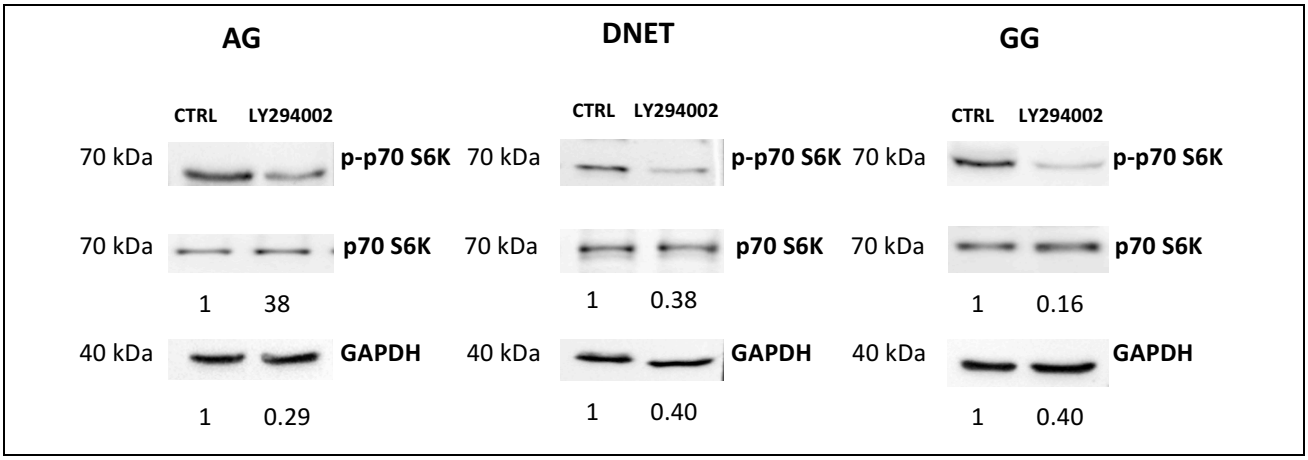

Figure 12. Phosphorylation of p70 S6K in pLGG cells subjected to LY294002 treatment. *The direct PI3K inhibition for 30 min with 50 μM LY294002 followed by a 48h recovery period in normal medium both strongly reduced p70 S6K phosphorylated levels (p-p70 S6K).*

These data indicate that the downregulated expression of miR-139-5p in primary supratentorial pLGG cells increases their proliferation by de-repressing PI3K/AKT signaling and that its effect is mediated by mTORC1, as summarized in Figure 13.

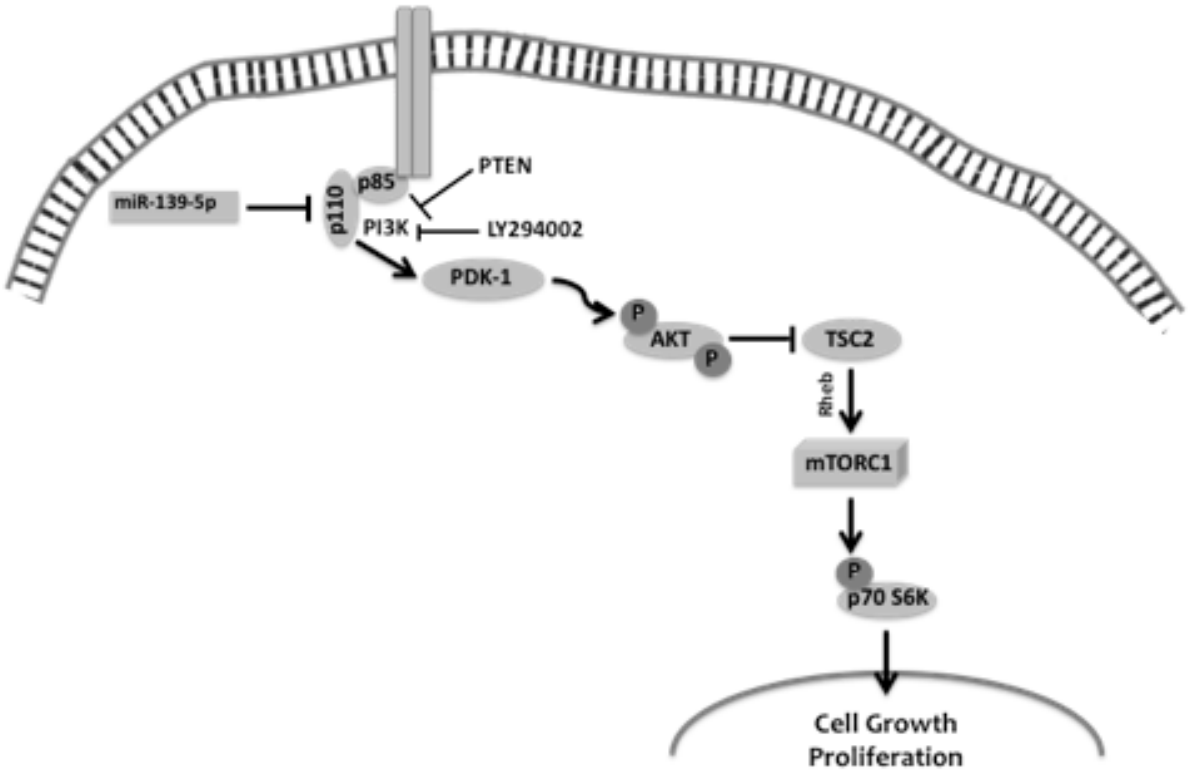

Figure 13. Downregulation of miR-139-5p expression in pLGGs promotes proliferation by de-repressing PI3K/AKT/mTORC1 signaling. *miR-139-5p, that targets the 3'-UTR of PIK3CA, is strongly downregulated in pLGG tumors resulting in the hyper-activation of the PI3K/AKT pathway. After miR-139-5p overexpression in pLGG primary cells both AKT and p70 S6K phosphorylation levels are reduced, with a consistent significant impairment in cell proliferation. PTEN, phosphatase and tensin homolog; PI3K, phosphatydil-inositol-3-kinase; PDK-1, phosphoinositide-dependent kinase 1; TSC2, tuberous sclerosis complex 2; Rheb, Ras homolog enriched in brain; mTORC1, mammalian target of rapamycin 1; p70 S6K, p70 S6 kinase.*

4.2 Evaluation of microRNAs as prognostic biomarkers in pLGGs

4.2.1 Cohort I microRNA profiling

All samples from Cohort I (19 supratentorial and 56 infratentorial PAs) were subjected to microRNA-seq analysis and relevant clinical data were collected (Table 5). STR *vs* GTR samples were compared and resulting in the identification of 151 differentially expressed (DE) microRNAs. Specifically, 110 microRNAs were upregulated and 41 downregulated in any residual (all STR in this cohort) *vs* GTR. It is worth noting that members of the miR-17-92 (miR-17-3p and miR-18a-3p) and miR-106b-25 (miR-106b-5p and miR-93-5p) clusters were identified among the up-regulated microRNAs. Hierarchical clustering analysis generated with DE microRNAs showed the segregation of GTR and STR PA patients in one main cluster and individual branches (Figure 14).

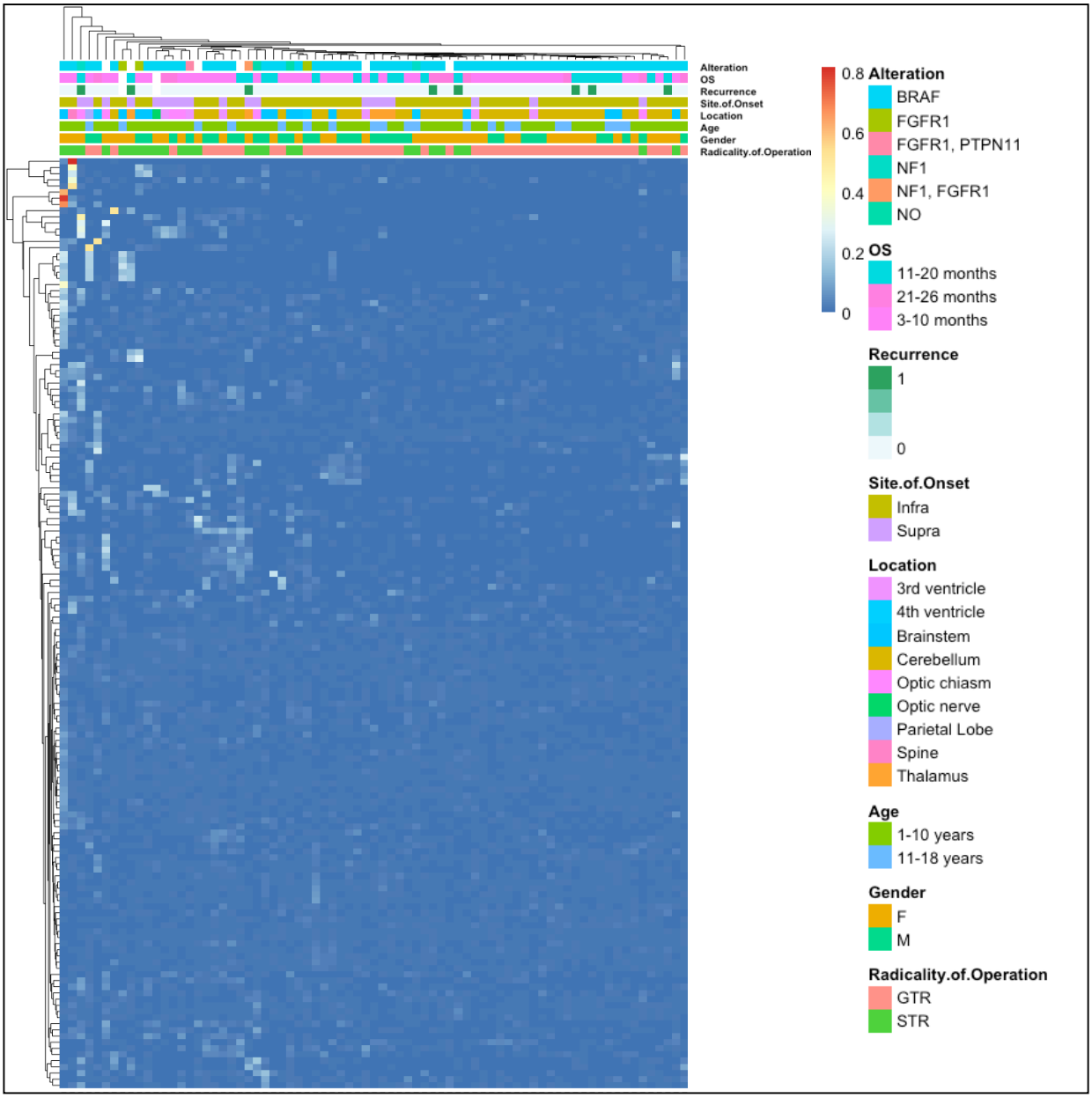

Figure 14. Hierarchical clustering of microRNAs displaying differential expression in PA that have undergone Gross Total Resection (GTR, pink) vs. PA that have undergone Sub Total Resection (STR, green) belonging to the first cohort (Cohort I). *Hierarchical clustering of the 151 microRNAs differentially expressed in PA that have undergone GTR (n=49) vs. PA that have undergone STR (n=26) (p<0.05) was performed and the bray method was used to generate clusters on the basis of RPM values.*

No correlation between clusters and tumor location, age, sex, mutational status and type of resection was observed. Thus, the comparison between any residual and GTR failed to segregate samples. The recurrence rate between any residual and GTR was investigated, observing a higher rate of recurrence in any residual (Figure 15A). Furthermore, among the any residual subgroup, the recurrence rate is even higher in the supratentorial subset (Figure 15B).

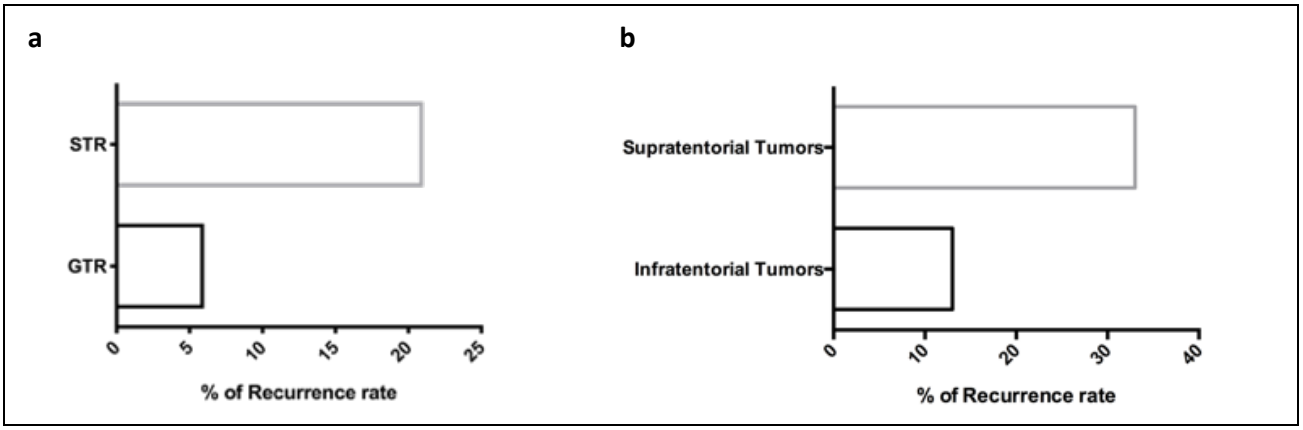

Figure 15. Analysis of the recurrence rate of tumors belonging to the first cohort (Cohort I). ***(a)*** *GTR samples showed a lower recurrence rate than STR.* ***(b)*** *Among the STR subset of samples, supratentorial tumors presented a higher recurrence rate than infratentorial ones.*

On the basis of the above reported evidences, the analysis was focused on the microRNA profiles of supratentorial-any residual samples considering two categories; with or without recurrence. The mean and the median age at diagnosis were 5.9 and 5 years old, respectively. Samples that experienced recurrence were located in the thalamus (n=2) and in the optic chiasm (n=1), while the ones that did not recur arose in the optic chiasm (n=4) and in the third ventricle (n=2). 32 microRNAs were upregulated, while 52 were downregulated in tumors with recurrence (Tables 7 and 8) and were used for hierarchical clustering analysis (Figure 16). Interestingly, the microRNA profile clearly distinguished tumors that underwent recurrence from the ones that did not.

Table 7. MicroRNAs displaying significantly upregulated expression in subtotally resected (STR) PAs with recurrence in respect to subtotally resected (STR) PAs without recurrence.

microRNA	LFC	P-value	Part of cluster	Chr
hsa-miR-1248	3,337	1,20E-02		
hsa-miR-1264	3,202	1,17E-02	1912~1264	X
hsa-miR-1298	1,957	4,41E-02		
hsa-miR-135a-3p	1,711	2,31E-03		
hsa-miR-135a-5p	2,294	4,33E-02		
hsa-miR-1912	3,194	1,35E-02	1912~1264	X
hsa-miR-194-5p	0,884	8,19E-03	194-1~215	1
hsa-miR-211-5p	2,677	2,17E-02		
hsa-miR-2467-3p	4,275	1,40E-02		
hsa-miR-30c-5p	0,849	3,77E-02	30e~30c-1	1
hsa-miR-30e-5p	0,823	3,86E-03	30e~30c-1	1
hsa-miR-34b-3p	1,189	3,92E-02	34b~34c	11
hsa-miR-34c-5p	1,358	4,77E-02	34b~34c	11
hsa-miR-3607-3p	1,996	1,34E-02		
hsa-miR-3607-5p	1,544	1,89E-03		
hsa-miR-3609	2,017	4,30E-02		
hsa-miR-3617	1,808	3,53E-02		
hsa-miR-3622a-5p	1,689	2,10E-04	3622a~3622b	8
hsa-miR-3622b-3p	2,503	2,37E-04	3622a~3622b	8
hsa-miR-3690	2,875	1,05E-04		
hsa-miR-3923	3,865	9,63E-04		
hsa-miR-3941	2,935	4,56E-02		
hsa-miR-4510	4,923	1,52E-07		
hsa-miR-4679	1,842	4,55E-02	4679-1~4679-2	10
hsa-miR-4711-3p	4,238	1,95E-02		
hsa-miR-518c-5p	4,777	4,74E-02	512-1~519a-2	19
hsa-miR-548ah-3p	2,497	1,02E-02	4450~548ah	4
hsa-miR-548k	0,907	2,86E-02		
hsa-miR-548p	2,423	1,24E-02		
hsa-miR-651	0,924	4,37E-02		
hsa-miR-92b-3p	0,912	2,64E-02		
hsa-miR-96-3p	3,798	4,77E-02	183~182	7

Table 8. MicroRNAs displaying significantly downregulated expression in supratentorial subtotally resected (STR) PAs with recurrence in respect to subtotally resected (STR) PAs without recurrence.

microRNA	LFC	P-value	Part of cluster	Chr
hsa-miR-125a-5p	-0,577	4,42E-02	99b~125a	19
hsa-miR-126-5p	-1,218	9,83E-03		
hsa-miR-1260a	-0,826	7,03E-03		
hsa-miR-1260b	-0,824	5,61E-03		
hsa-miR-1277-5p	-1,197	3,15E-02		
hsa-miR-1299	-2,644	6,15E-03		
hsa-miR-1307-3p	-0,671	1,61E-02		
hsa-miR-132-3p	-1,632	3,87E-02	212~132	17
hsa-miR-136-5p	-1,192	2,33E-02	493~136	14
hsa-miR-143-5p	-1,589	9,29E-03	143~145	5
hsa-miR-1538	-1,799	2,08E-02		
hsa-miR-187-3p	-2,377	1,25E-02		
hsa-miR-21-3p	-1,541	1,63E-02		
hsa-miR-210	-2,143	1,44E-02		
hsa-miR-212-3p	-1,882	1,52E-02	212~132	17
hsa-miR-214-5p	-1,445	3,53E-02	199a-2~214	1
hsa-miR-219-5p	-2,313	4,77E-02		
hsa-miR-29b-1-5p	-1,184	2,19E-03	29b-1~29a	7
hsa-miR-3123	-6,214	8,18E-03		
hsa-miR-3142	-6,778	2,12E-03		
hsa-miR-3162-3p	-5,354	1,50E-02		
hsa-miR-3529-5p	-1,768	3,76E-02	1179~3529	15
hsa-miR-361-5p	-0,745	4,60E-02		
hsa-miR-3612	-2,131	1,55E-02		
hsa-miR-370	-1,098	3,92E-02		
hsa-miR-376a-3p	-1,357	2,88E-02	379~656	14

hsa-miR-376b	-1,134	3,94E-02	379~656	14
hsa-miR-377-5p	-1,111	5,19E-03	379~656	14
hsa-miR-3922-5p	-2,422	1,05E-02		
hsa-miR-423-5p	-0,817	4,43E-02	423~3184	17
hsa-miR-4418	-4,733	3,75E-02		
hsa-miR-4458	-5,560	4,02E-03		
hsa-miR-4502	-4,791	3,57E-02		
hsa-miR-4697-3p	-2,097	3,84E-02		
hsa-miR-4705	-2,040	1,63E-02		
hsa-miR-4754	-2,570	4,97E-02		
hsa-miR-4758-3p	-2,990	1,54E-02		
hsa-miR-4768-5p	-2,523	1,60E-02		
hsa-miR-544b	-4,714	1,62E-02		
hsa-miR-5587-3p	-3,433	2,05E-02	5587~3176	16
hsa-miR-5699	-0,956	1,97E-02		
hsa-miR-574-5p	-1,837	6,35E-03		
hsa-miR-602	-2,770	3,44E-02		
hsa-miR-616-3p	-1,393	2,03E-02	6758~616	12
hsa-miR-638	-5,119	2,16E-02		
hsa-miR-671-5p	-1,199	2,64E-02		
hsa-miR-766-5p	-1,524	1,63E-02		
hsa-miR-875-3p	-4,766	4,12E-02	875~599	8
hsa-miR-888-5p	-2,426	7,73E-03	891b~892c	X
hsa-miR-890	-2,496	3,59E-02	891b~892c	X
hsa-miR-892a	-2,115	4,82E-02	891b~892c	X
hsa-miR-892b	-3,147	7,70E-03	891b~892c	X

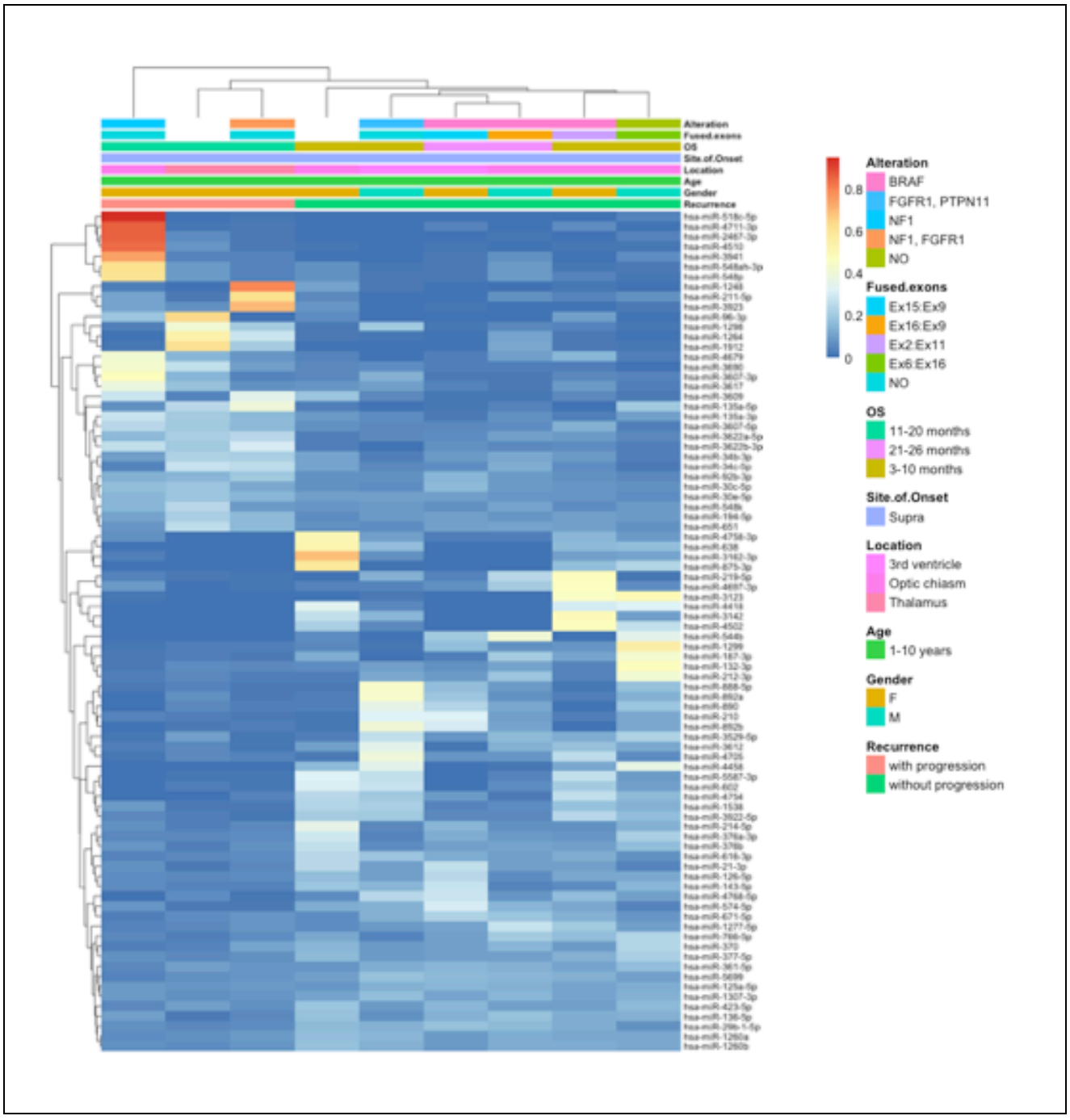

Figure 16. Hierarchical clustering of microRNAs displaying differential expression in supratentorial PA with recurrence (pink) vs. supratentorial PA without recurrence (green) belonging to the first cohort (Cohort I). *Hierarchical clustering of the 84 microRNAs differentially expressed in supratentorial PA with recurrence (n=3) vs. supratentorial PA (n=6) without recurrence (p<0.05) was performed and the bray method was used to generate clusters on the basis of RPM values.*

4.2.2 Cohort II microRNA profiling

MicroRNA profiling disclosed a higher number of detected microRNAs in the subgroup without recurrence (53%) with respect to tumors with recurrence (44%). Differential expression analyses resulted in 29 microRNAs, five upregulated and 24 downregulated in tumors with recurrence versus without recurrence (Figure 17). The hierarchical clustering clearly distinguished the two subgroups of patients (Figure 18): one branch included only tumors with recurrence and the second main branch was further subdivided in a branch with only pLGGs without recurrence and a branch with mixed samples. It is worth noting that in each branch there was also a distinction on the basis of the site of onset of tumors. This result underlines that DE microRNAs reflect at least in part the distinct embryologic origin between tumors, hemispheric or midline respectively.

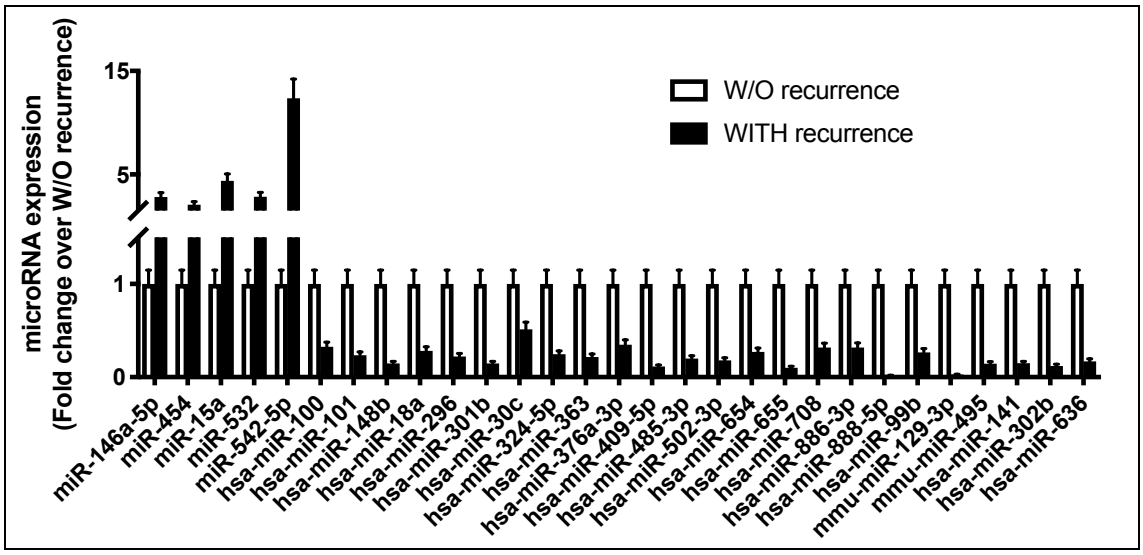

Figure 17. Differentially expressed microRNAs in partially resected (PR) pLGGs belonging to the second cohort (Cohort II). *Five microRNAs were significantly upregulated and twenty-four were significantly down-regulated in PR pLGGs that experienced recurrence (WITH recurrence) in respect to pLGGs without recurrence (W/O recurrence).*

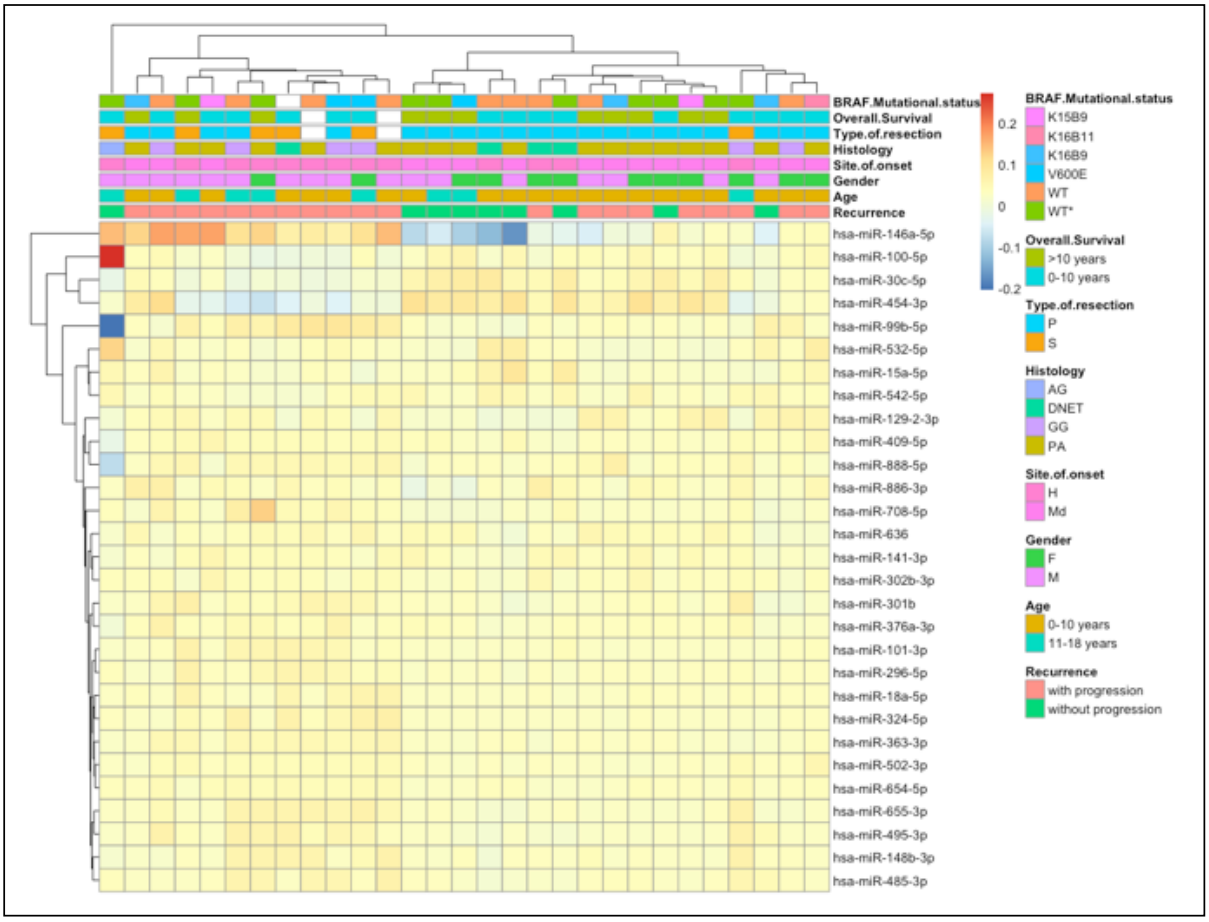

Figure 18. Hierarchical clustering of microRNAs displaying differential expression in pLGGs with recurrence (pink) vs. pLGG without recurrence (green) belonging to the second cohort (Cohort II). *Hierarchical clustering of the 29 microRNAs differentially expressed in pLGGs with recurrence (n=20) vs. pLGG without recurrence (n=9) (p<0.05) was performed and the bray method was used to generate clusters on the basis of delta Ct values.*

4.2.3 MicroRNAs as prognostic biomarkers in pLGGs from both cohorts

With the aim to identify microRNAs that can stratify patients into prognostic risk categories, the results obtained from Cohorts I and II were compared and the commonly deregulated microRNAs were examined. Of note, even though Cohort I comprised only midline PAs tumors and Cohort II both midline and hemispheric samples belonging to different histotypes, two microRNAs, miR-376a-3p and miR-888-5p, were commonly downregulated in pLGGs that experienced recurrence (Figure 19A).

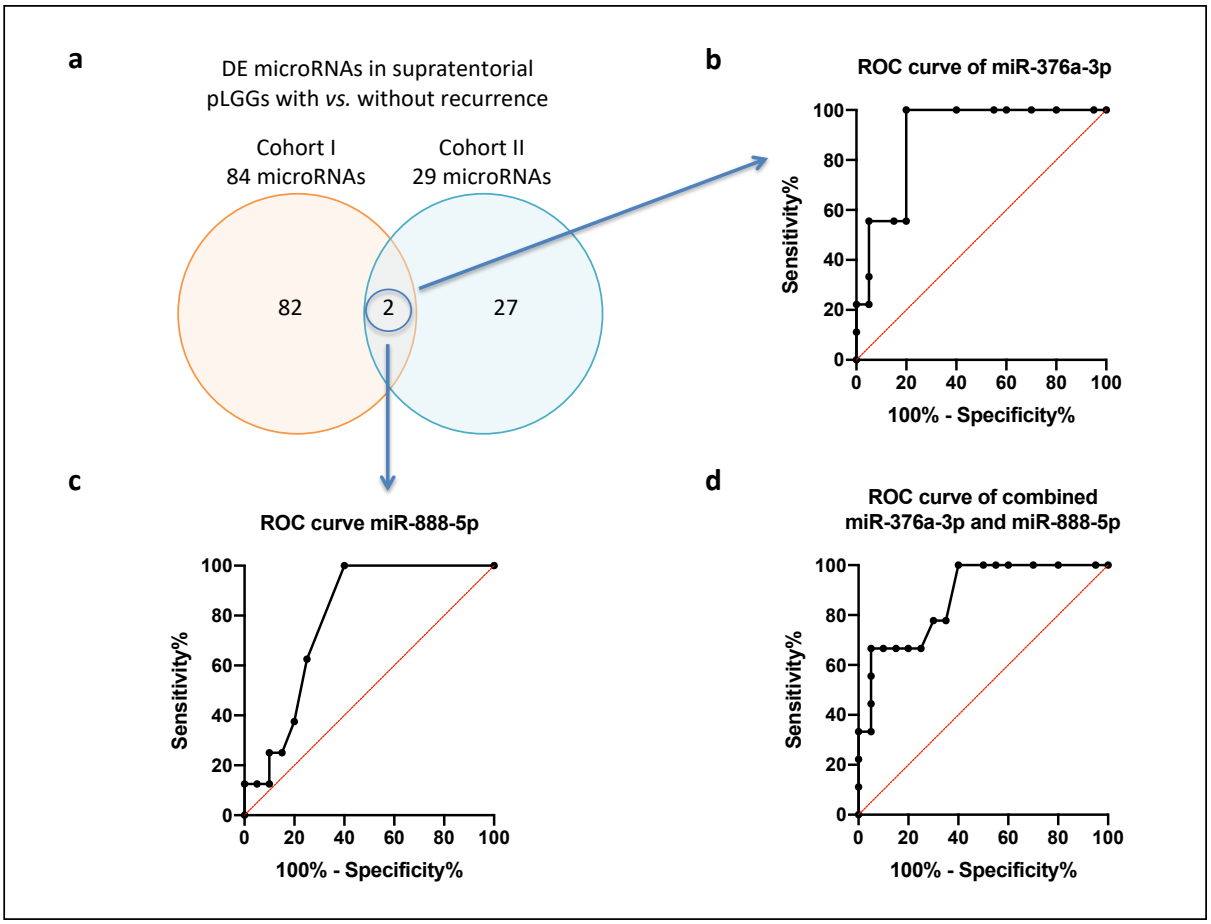

Figure 19. Identification of microRNAs as prognostic biomarkers. ***(a)*** *Venny diagram of DE microRNAs in supratentorial pLGGs with vs. without recurrence (Cohort I in orange, Cohort II in blue). ROC curves of the proposed microRNA signature:* ***(b)*** *ROC curves of miR-376a-3p (AUC=0.8944, p=0.0008),* ***(c)*** *miR-888-5p (AUC=0.7875, p=0.0193) and* ***(d)*** *the combination of the two microRNAs (AUC=0.8694, p=0.0017). Black line=sensitivity, red line=identity.*

Univariate analysis was performed for each microRNA taking into consideration the available clinical data for each cohort (significant results in Table 9).

Table 9 Univariate analyses of miR-376a-3p (A) and miR-888-5p (B) by PFS and other clinical features in pLGG.

(A)

Validation cohort - Univariate analysis for miR-376a-3p

UNIANOVA miR-376a-3p BY SiteOfOnset Histology Age WITH Recurrence

Tests of Between-Subjects Effects

Dependent Variable:	miR376a							
Source	Type III Sum of Squares	df	Mean Square	F*	Sig.	Partial Eta Squared $	Noncent. Parameter	Observed Power b
Corrected Model	58.076 a	13,000	4,467	3,702	0,013	0,787	48,121	0,920
Histology	16,364	3,000	5,455	4,520	**0,022**	0,511	13,559	0,762
Error	15,689	13,000	1,207					
Total	738,349	27,000						
Corrected Total	73,765	26,000						

a. R Squared = .787 (Adjusted R Squared = .575)

*. F-value is the Mean Square Regression divided by the Mean Square Residual

$. proportion of variance accounted for by some effect

b. Computed using alpha = .05

Parameter Estimates

Dependent Variable:	miR376a								
					95% Confidence				
Parameter	B c	Std. Error	t	Sig.	Lower Bound	Upper Bound	Partial Eta Squared$	Noncent. Parameter	Observed Power b
[SiteOfOnset=H]	3,626	1,627	2,228	**0,044**	0,111	7,141	0,276	2,228	0,541
[Histology=AG]	-4,511	1,563	-2,886	**0,013**	-7,888	-1,134	0,390	2,886	0,760
[Histology=GG]	5,255	1,276	4,120	**0,001**	2,500	8,011	0,566	4,120	0,967
[SiteOfOnset=H] * [Histology=GG]	-6,336	1,870	-3,388	**0,005**	-10,375	-2,296	0,469	3,388	0,879

a. This parameter is set to zero because it is redundant.

b. Computed using alpha = .05

c. Unstandardized coefficients

B)

Discovery cohort - Univariate analysis for miR-888-5p

UNIANOVA miR-888-5p BY SiteOfOnset Histology Alterations Age WITH Recurrence

Tests of Between-Subjects Effects

Dependent Variable:

Source	Type III Sum of Squares	df	Mean Square	F*	Sig.	Partial Eta Squared$	Noncent. Parameter	Observed Power[b]
Corrected Model	1172444.753[a]	5,000	234488,951	17,913	0,019	0,968	89,565	0,887
Intercept	135411,146	1,000	135411,146	10,344	0,049	0,775	10,344	0,586
PFS	310648,584	1,000	310648,584	23,731	**0,017**	0,888	23,731	0,885
Age	278118,994	1,000	278118,994	21,246	**0,019**	0,876	21,246	0,853
Age * Gender	375641,167	1,000	375641,167	28,696	**0,013**	0,905	28,696	0,930
Error	39271,228	3,000	13090,409					
Total	2097742,845	9,000						
Corrected Total	1211715,980	8,000						

a. R Squared = .968 (Adjusted R Squared = .914)

*. F-value is the Mean Square Regression divided by the Mean Square Residual

$. proportion of variance accounted for by some effect

b. Computed using alpha = .05

Parameter Estimates

Dependent Variable:

Parameter	B[c]	Std. Error	t	Sig.	95% Confidence Interval		Partial Eta Squared$	Noncent. Parameter	Observed Power [b]
					Lower Bound	Upper Bound			
Intercept	332,865	137,243	2,425	0,094	-103,903	769,634	0,662	2,425	0,389
PFS	83,086	17,056	4,871	**0,017**	28,807	137,365	0,888	4,871	0,885
[Age=<5]	-1913,680	299,205	-6,396	**0,008**	-2865,885	-961,475	0,932	6,396	0,980
[Age=>5]	0[a]								
[Gender=F]	-1732,868	257,112	-6,740	**0,007**	-2551,113	-914,622	0,938	6,740	0,988
[Age=<5] *	2993,514	558,819	5,357	**0,013**	1215,102	4771,927	0,905	5,357	0,930
[Age=<5]	0[a]								

a. This parameter is set to zero because it is redundant.

b. Computed using alpha = .05

c. Unstandardized coefficients

In detail, univariate analysis of miR-376a-3p did not account for any significant features in Cohort I (consisting of only PAs), while Site of Onset, Histology and the combination of Histology and Site of Onset were significant for miR-376a-3p in Cohort II. This result is consistent with Cohort I, consisting of PAs with Midline Site of Onset.

Univariate analysis of miR-888-5p reports PFS, Age and the combination of Age and Gender as significant factors in Cohort I, whereas no feature was significant in Cohort II. The Cohort I result can be explained by the fact that 55% of patients with progression are younger than 5 years old and 66% of patients with progression are female.

These result underline that the two microRNAs are not associated with the different embryologic origin of these tumors or with the histotypes and can be used as universal prognostic biomarkers for pLGGs.

Subsequently, we performed ROC analysis in order to evaluate the prognostic potential of these microRNAs as biomarkers. We investigated miR-376a-3p and miR-888-5p AUC and p-value singularly and after their combination. Both of them showed a high specificity and sensitivity in distinguishing between PR patients that presented or not tumor recurrence, both separately and in combination (Figure 19 B-D).

In situ analysis of microRNA expression was performed for miR-376a-3p and miR-888-5p with ISH in a subset of different tumors histotypes. The number of positive neoplastic cells for both microRNAs was significantly higher in tumor without recurrence ($p<0.0001$ for miR-376a-3p, $p<0.05$ for miR-888-5p). Noteworthy, a positive staining was detectable in tumor cells and in neurons, while normal glial cells were negative (data not shown). miR-376a-3p and miR-888-5p were localized both into the nucleus and cytoplasm of neoplastic cells (Figure 20 and 21).

These data validate the results obtained by both microRNA profiling technologies in the two cohorts.

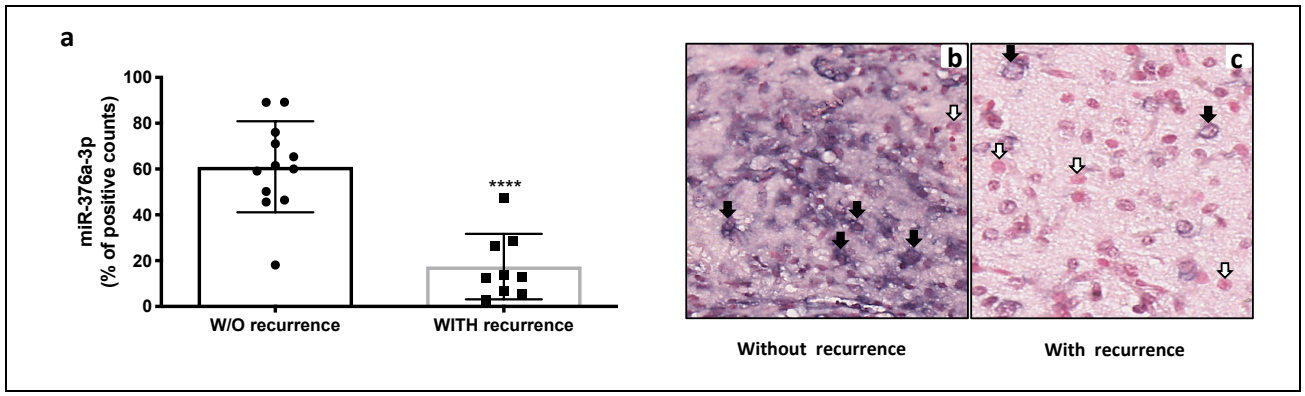

Figure 20. miR-376a-3p in pLGG with and without recurrence.

(a) *Percentage of positive counts is reported, relative to the total count measured. * p<0.0001 vs W/O progression.*
(b, c) *Representative images of ISH on pLGG samples with* ***(C)*** *and without recurrence* ***(B)*** *that confirm the higher expression of miR-376a-3p in samples without recurrence.*
(b) *PA. The signal of miR-376a-3p is clearly detectable in the neoplastic cells (black arrows), where it shows a nucleus and a cytoplasmic staining with an intense perinuclear enhancement. The microRNA expression exhibits a diffuse staining. Rare neoplastic cells are negative for miR-376a-3p (white arrow).*
(c) *GG. The expression of miR-376a-3p shows a fainty blue staining both into the nucleus and the cytoplasm of neoplastic cells (black arrows). Many neoplastic cells are negative (white arrows). Original Magnification 40X, Bars 20 µm.*

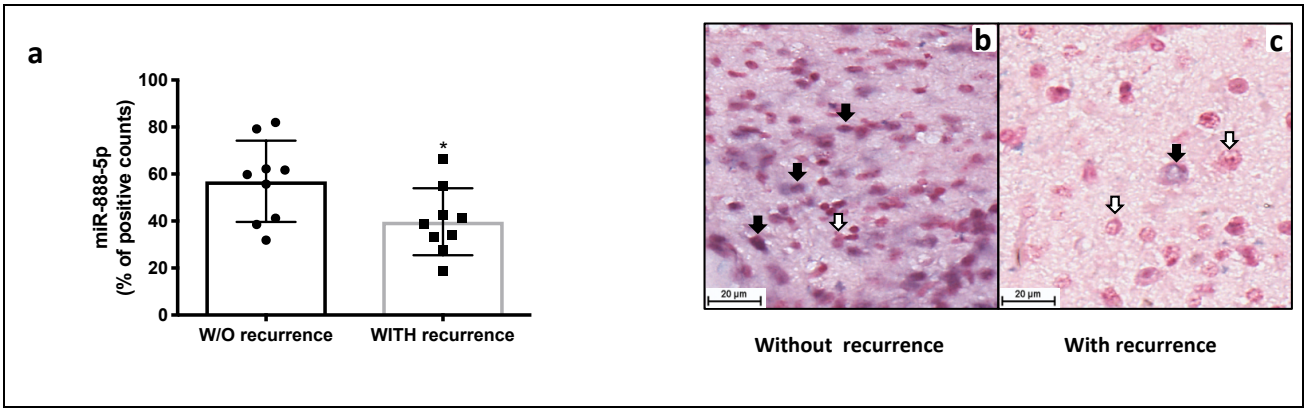

Figure 21. miR-888-5p in pLGG with and without recurrence.

(a) *Percentage of positive counts is reported, relative to the total count measured. * p<0.05 vs W/O progression.*
(b, c) *Representative images of ISH on pLGG samples with* ***(C)*** *and without recurrence* ***(B)*** *that confirm the higher expression of miR-888-5p in the sample without recurrence.*
(b) *PA. The signal of miR-888-5p is evident in the cytoplasm and in the nucleus of neoplastic cells (black arrows) with a mild expression. The blue staining shows a dotted pattern. Some neoplastic cells are negative for miR-888-5p (white arrow)*
(c) *GG. The expression of miR-888-5p shows a weak blue staining in rare neoplastic cells (black arrow) with a cytoplasmic and nuclear pattern of staining, while many neplastic cells are negative (white arrow). Original Magnification 40X, Bars 20 µm.*

4.2.4 miR-376a-3p and miR-888-5p enrichment analysis

In order to gain insight into the role of miR-376a-3p and miR-888-5p in pLGGs, disease enrichment analysis was performed. First, the targets of miR-376a-3p and miR-888-5p were queried and 662 and 425 genes were obtained, respectively. Among them, 32 were common targets of both microRNAs. Using the two microRNAs and the 32 genes enriched pathways were obtained and the 30 categories with the highest numbers of molecules involved were reported in Table 10. The categories of interest included: Extracranial solid tumor, High grade astrocytoma, Grade 4 high grade glioma, Grade 4 malignant gliomas, Grade 4 astrocytoma and Brain astrocytoma. Further investigation of the genes that were present in at least two of the above mentioned categories lead to the query of the following genes Defensin Beta 132 (DEFB132), ELOVL fatty acid elongase 7 (ELOVL7), Fibroblast growth factor 14 (FGF14), Interleukin 15 (IL15) and Zinc finger protein 714 (ZNF714) (Table 11). Investigation on the biological processes of these genes reported molecular functions, such as innate immune response, protein binding, growth factor activity, cytokine activity and regulation of transcription. It can be hypothesized that low microRNA expression failing to repress these genes is a possible mechanism for tumor growth and cancer invasion.

Thus, the enrichment analysis allowed the identification of candidates that could explain the functional role of miR-376a-3p and miR-888-5p in pLGG progression and further experiments are required to fully investigate the role and mechanism of action of these molecules in pLGG.

Table 10. Disease enrichment pathway analysis of microRNAs of interest - IPA analysis.

Categories	Diseases or Functions Annotation	p-value	Molecules	# Molecules
Cancer,Organismal Injury and Abnormalities	Carcinoma	3,16E-03	CHUK,DEFB132,EID2,EIF1B,ELOVL7,ERMN,FGF14,GCSAML,GRIN2B,HACD2,HIKESHI,IL15,KCNJ6,KPNA4,LILRA2,MEPE, miR-376a-3p (and other miRNAs w/seed	30
Cancer,Organismal Injury and Abnormalities	Extracranial solid tumor	9,29E-03	CHUK,DEFB132,EID2,EIF1B,ELOVL7,ERMN,FGF14,GCSAML,GRIN2B,HACD2,HIKESHI,IL15,KCNJ6,KPNA4,LILRA2,MEPE, miR-376a-3p (and other miRNAs w/seed	30
Cancer,Gastrointestinal Disease,Organismal Injury and Abnormalities	Digestive organ tumor	4,58E-03	CHUK,DEFB132,EIF1B,ERMN,FGF14,GCSAML,GRIN2B,HACD2,HIKESHI,IL15,KCNJ6,KPNA4,LILRA2,MEPE,miR-376a-3p (and other miRNAs w/seed	28
Cancer,Organismal Injury and Abnormalities	Abdominal cancer	1,23E-02	CHUK,DEFB132,EIF1B,ELOVL7,ERMN,FGF14,GCSAML,GRIN2B,HACD2,HIKESHI,IL15,KCNJ6,KPNA4,LILRA2,MEPE,miR-376a-3p (and other miRNAs w/seed	28
Cancer,Organismal Injury and Abnormalities	Abdominal carcinoma	1,91E-02	CHUK,DEFB132,EIF1B,ERMN,FGF14,GCSAML,GRIN2B,HACD2,HIKESHI,IL15,KCNJ6,KPNA4,LILRA2,MEPE,miR-376a-3p (and other miRNAs w/seed	27
Cancer,Gastrointestinal Disease,Organismal Injury and Abnormalities	Gastrointestinal tract cancer	6,09E-03	CHUK,DEFB132,EIF1B,FGF14,GCSAML,GRIN2B,HACD2,IL15,KCNJ6,KPNA4,LILRA2,MEPE,miR-376a-3p (and other miRNAs w/seed	26
Cancer,Organismal Injury and Abnormalities	Adenocarcinoma	2,50E-02	CHUK,DEFB132,EID2,EIF1B,ERMN,FGF14,GCSAML,GRIN2B,HACD2,KCNJ6,KPNA4,LILRA2,MEPE,miR-376a-3p (and other miRNAs w/seed	26
Cancer,Gastrointestinal Disease,Organismal Injury and Abnormalities	Malignant neoplasm of large intestine	8,08E-03	CHUK,DEFB132,EIF1B,FGF14,GCSAML,GRIN2B,HACD2,IL15,KCNJ6,KPNA4,LILRA2,MEPE,miR-376a-3p (and other miRNAs w/seed UCAUAGA),RAB30,RNF103,RXYLT1,SCAF11,ST6GAL2,SYT4,TMTC4,VMA21,ZFP14,ZNF460,ZNF667,ZNF714	25
Cancer,Organismal Injury and Abnormalities	Abdominal adenocarcinoma	4,34E-02	CHUK,DEFB132,EIF1B,ERMN,FGF14,GCSAML,GRIN2B,HACD2,KCNJ6,KPNA4,LILRA2,MEPE,miR-376a-3p (and other miRNAs w/seed	25
Cancer,Organismal Injury and Abnormalities	Malignant genitourinary solid tumor	2,77E-02	CHUK,DEFB132,EIF1B,ELOVL7,ERMN,GCSAML,GRIN2B,HIKESHI,IL15,KCNJ6,KPNA4,LILRA2,MEPE,miR-376a-3p (and other miRNAs w/seed UCAUAGA),RNF103,SCAF11,ST6GAL2,SYT4,ZFP14,ZNF667,ZNF714	21
Cancer,Organismal Injury and Abnormalities	Incidence of tumor	4,37E-02	CHUK,DEFB132,EID2,ERMN,GCSAML,GRIN2B,HACD2,IL15,KCNJ6,KPNA4,MEPE,RAB30,RNF103,SCAF11,ST6GAL2,SYT4, TMTC4,ZFP14,ZNF460,ZNF667,ZNF714	21
Cancer,Organismal Injury and Abnormalities	Genitourinary carcinoma	2,76E-02	CHUK,DEFB132,EIF1B,ERMN,GCSAML,GRIN2B,HIKESHI,IL15,KCNJ6,KPNA4,LILRA2,MEPE,RNF103,SCAF11,ST6GAL2,SY T4,ZFP14,ZNF667,ZNF714	19
Molecular Transport	Transport of molecule	5,82E-03	CHUK,FGF14,GRIN2B,HIKESHI,IL15,KCNJ6,KPNA4,RAB27B,SYT4	9
Cancer,Endocrine System Disorders,Gastrointestinal Disease,Organismal Injury and Abnormalities	Pancreatic ductal adenocarcinoma	3,16E-02	CHUK,DEFB132,GCSAML,miR-376a-3p (and other miRNAs w/seed UCAUAGA),RNF103,TMTC4,ZNF460,ZNF667	8
Metabolic Disease,Organismal Injury and Abnormalities	Glucose metabolism disorder	3,40E-02	CHUK,FGF14,GRIN2B,HACD2,IL15,ISCA1,KCNJ6	7
Endocrine System Disorders,Gastrointestinal Disease,Metabolic Disease,Organismal Injury and	Diabetes mellitus	4,15E-02	CHUK,FGF14,GRIN2B,HACD2,IL15,KCNJ6	6
Cancer,Neurological Disease,Organismal Injury and Abnormalities	High grade astrocytoma	3,21E-02	DEFB132,ELOVL7,FGF14,IL15,ZNF714	5
Cardiovascular Disease,Organismal Injury and	Peripheral vascular disease	1,16E-02	EIF1B,GRIN2B,IL15,MEPE	4
Cancer,Neurological Disease,Organismal Injury and Abnormalities	Grade 4 high grade glioma	2,39E-02	DEFB132,ELOVL7,FGF14,ZNF714	4
Cancer,Neurological Disease,Organismal Injury and Abnormalities	Grade 4 malignant glioma	2,39E-02	DEFB132,ELOVL7,FGF14,ZNF714	4
Cancer,Neurological Disease,Organismal Injury and Abnormalities	Grade 4 astrocytoma	2,39E-02	DEFB132,ELOVL7,FGF14,ZNF714	4
Cancer,Neurological Disease,Organismal Injury and Abnormalities	Brain astrocytoma	2,58E-02	DEFB132,ELOVL7,FGF14,ZNF714	4
Connective Tissue Disorders,Organismal Injury and Abnormalities,Skeletal and Muscular Disorders,Tissue Morphology	Damage of bone	2,67E-03	GRIN2B,IL15,MEPE	3
Nervous System Development and Function	Coordination	6,72E-03	GRIN2B,RNF103,SYT4	3
Behavior	Conditioning	6,78E-03	GRIN2B,RNF103,SYT4	3
Behavior	Anxiety	6,78E-03	GRIN2B,KCNJ6,RNF103	3
Hereditary Disorder,Neurological Disease,Organismal Injury and Abnormalities	Autosomal dominant encephalopathy	1,40E-02	FGF14,GRIN2B,KCNJ6	3
Behavior,Nervous System Development and Function	Memory	1,62E-02	CHUK,GRIN2B,SYT4	3
Cellular Movement,Hematological System Development and Function,Immune Cell Trafficking,Inflammatory	Cell movement of macrophages	1,82E-02	CHUK,IL15,KPNA4	3
Molecular Transport	Transport of metal ion	1,84E-02	FGF14,GRIN2B,KCNJ6	3

Table 11. Disease specific function of the molecules targeted by miR-376a-3p and miR-888-5p.

Molecules of interest	Official Full Name	Description of molecule	General Molecular function and Biological process	Reference
DEFB132	Defensin Beta 132	Defensins are cysteine-rich cationic polypeptides that are important in the immunologic response to invading microorganisms.	defense response to Gram-negative bacterium; innate immune response; killing of cells of other organism	National Center for Biotechnology Information (NCBI)[Internet]. Bethesda (MD): National Library of Medicine (US), National Center for Biotechnology Information; [1988] – [cited 2017 Apr 06]. Available from: https://www.ncbi.nlm.nih.gov/
ELOVL7	ELOVL fatty acid elongase 7	Catalyzes the first and rate-limiting reaction of the four reactions that constitute the long-chain fatty acids elongation cycle. May participate in the production of saturated and polyunsaturated VLCFAs of different chain lengths that are involved in multiple biological processes as precursors of membrane lipids and lipid mediators.	fatty acid elongase activity; protein binding; transferase activity	National Center for Biotechnology Information (NCBI)[Internet]. Bethesda (MD): National Library of Medicine (US), National Center for Biotechnology Information; [1988] – [cited 2017 Apr 06]. Available from: https://www.ncbi.nlm.nih.gov/ ; The UniProt Consortium UniProt: a worldwide hub of protein knowledge Nucleic Acids Res. 47: D506-515 (2019)
FGF14	Fibroblast growth factor 14	FGF family members possess broad mitogenic and cell survival activities, and are involved in a variety of biological processes, including embryonic development, cell growth, morphogenesis, tissue repair, tumor growth and invasion.	fibroblast growth factor receptor binding; growth factor activity; heparin binding; protein binding	National Center for Biotechnology Information (NCBI)[Internet]. Bethesda (MD): National Library of Medicine (US), National Center for Biotechnology Information; [1988] – [cited 2017 Apr 06]. Available from: https://www.ncbi.nlm.nih.gov/
IL15	Interleukin 15	The protein encoded by the IL15 gene is a cytokine that regulates T and natural killer cell activation and proliferation. This cytokine induces the activation of JAK kinases, as well as the phosphorylation and activation of transcription activators STAT3, STAT5, and STAT6.	cytokine activity; cytokine receptor binding; protein binding	National Center for Biotechnology Information (NCBI)[Internet]. Bethesda (MD): National Library of Medicine (US), National Center for Biotechnology Information; [1988] – [cited 2017 Apr 06]. Available from: https://www.ncbi.nlm.nih.gov/
ZNF714	Zinc finger protein 714	May be involved in transcriptional regulation.	regulation of transcription, DNA-dependent	National Center for Biotechnology Information (NCBI)[Internet]. Bethesda (MD): National Library of Medicine (US), National Center for Biotechnology Information; [1988] – [cited 2017 Apr 06]. Available from: https://www.ncbi.nlm.nih.gov/ ; The UniProt Consortium UniProt: a worldwide hub of protein knowledge Nucleic Acids Res. 47: D506-515 (2019)

5. Discussion

Pediatric low-grade gliomas (pLGGs) are a heterogeneous group of grade I and II glial tumors. pLGGs are treated with complete surgical resection; however, if not feasible, patients receive chemotherapy and, in case of older children, radiotherapy with a PFS rate in the range of 30-40% after 5 years [82,83]. Residual disease and/or treatments cause significant morbidity [84]. Recent studies indeed investigated genetic alterations as a tool for the stratification of pLGG patients into risk categories with the aim of contributing in clinical decisions and underlined the need for multiple molecular biomarkers to better define the clinical management of these tumors [5,6]. Since morbidity and mortality, particularly due to disease progression, represent a significant problem in children affected by pLGGs even after many years from diagnosis [26,9,85] there is an urgent need:

-for the identification and use of less toxic therapies, such as molecular targeted agents, in children with LGGs and

-for the identification of diagnostic and prognostic biomarkers, such as epigenetic prognostic biomarkers able to predict if pLGG patients will go into progression when complete surgical resection is not feasible and will need chemo and/or radiotherapy, from patients that will not progress.

MicroRNAs act as pivotal players in gene regulation and their deregulation has been described in pLGGs as well as in other solid tumors [86]. Numerous studies have confirmed that overexpression of microRNAs has the potential to promote cancer development. Intriguingly, some miRNAs have been identified to exert anticancer effects. Thus, defined interrogations of the oncogenic microRNAs (oncomiRs) that can lead to irregularities of gene expression or enhancement of tumor suppressor miRNAs might become potential therapeutic approaches. Additionally, the tissue specificity of microRNA expression may be useful to identify different tumor types and the tissue of origin [87]. Consequently, they are optimal candidates as diagnostic and prognostic biomarkers [88].

Thus far, however, the research conducted on these noncoding RNA species in pLGGs has been largely descriptive. Moreover, the conclusions that can be drawn from these studies are frequently limited by the small number of samples analyzed [55,58] the inclusion of high-grade gliomas besides pLGGs [53,57] or the inclusion of adult patients [61].

In this context of microRNAs evaluation in pLGG tumors, this study aimed to identify new molecular aspects in pLGG patients by investigating the functional and prognostic role of some deregulated microRNAs with particular interest. This study addressed two main aims, the first was to perform experiments that would further support the development of targeted biological therapies with microRNAs that play a role in supratentorial pLGGs, in order to reduce morbidity related to chemo and/or radiotherapy treatment. The second aim was to identify microRNAs with prognostic value in supratentorial pLGGs, patients with worse prognosis not amenable to complete surgical resection.

Firstly, the study focused on the functional role of miR-139-5p in pLGGs. Thanks to previously published data of microRNA expression profiling between samples of supratentorial pLGG patients tissue and samples of healthy brain tissue [70], the downregulation of miR-139-5p in pLGGs was reported and its functional role in the activation of PI3K/AKT/mTORC1 signaling was investigated. This microRNA is a known regulator of the *PIK3CA* gene, which encodes the catalytic subunit of the PI3K. The importance of the PI3K/AKT/mTORC1 pathway in pLGGs is well reported by different studies that demonstrate its upregulation [3,7,89,90]. The oncosuppressive effects of miR-139-5p have been described in a variety of solid tumors [91-95], including adult and pediatric high-grade gliomas [96,97,76]. Nonetheless, the expression of miR-139-5p has only been explicitly investigated in pLGGs in one study and extension of these results with new samples was necessary. The functional characterization of miR-139-5p loss in grade I pLGGs provides the evidence that this alteration may be a key driver of oncogenic activation of the PI3K/AKT/mTORC1 pathway in these tumors. As illustrated in Figure 13, the downregulated miR-139-5p expression in supratentorial pLGGs significantly enhances activation of PI3K/AKT/mTORC1 signaling, as reflected by the high phosphorylation levels of AKT and p70 S6K, which dropped markedly after miR-139-5p overexpression, and the biological outcome is a substantial increase in tumor-cell proliferation. It is also important to recall that miR-139-5p downregulation might produce additional tumor-promoting effects by derepressing other targets, which include numerous genes with documented oncogenic effects in gliomas and in other cancers as well (e.g., FOS, HRAS, JUN, MCL1, NOTCH1, ELTD1, ZEB1 and ZEB2) [89,92-94,96,97]. These conclusions are based on results obtained from the restored expression of miR-139-5p in primary cultures of patient-derived supratentorial pLGG cells, whereas the few functional studies that have been conducted in this area have utilized immortalized pLGG cells. In summary, the identification of miR-139-5p as a major regulator of the

PI3K/AKT/mTORC1 axis in supratentorial pLGGs and its evaluation in patients'-derived cellular models represent an important advancement deepening the current knowledge on pLGGs biology. Secondly, in the context of biomarkers, the research was focused on the identification of epigenetic prognostic biomarkers able to predict pLGG patient's recurrence in the absence of a complete surgical resection.

Initially, the microRNA expression profile of a cohort of completely and incompletely resected infratentorial and supratentorial pLGG patients was investigated. Comparison of the microRNA profile in a wide cohort of infratentorial and supratentorial PA subjected to GTR or STR was performed and the significant up-regulation of microRNAs with a known oncogenic role was observed (e.g. miR-17-3p, miR-18a-3p, miR-106b-5p and miR-93-5p) [98] in the STR subgroup. However, the extent of the resection was not a determinant factor for the segregation of these tumors. Then, the research was specifically focused on shedding light on possible microRNA involvement in the incompletely resected supratentorial subset of patients. Indeed, since these patients present higher recurrence rate than the infratentorial subset, they need further molecular characterization to identify specific therapeutic targets. Moreover, previous studies demonstrated different microRNA profiles [70] and molecular features [99] between supratentorial and infratentorial pLGGs. In order to define microRNAs that can be used as prognostic biomarkers and may help in defining the correct treatment strategy for supratentorial STR and PR pLGGs, the microRNA profile of STR and/or PR pLGGs patients that underwent progression or not was investigated. Therefore, by focusing on supratentorial incompletely resected pLGGs, two microRNAs that can stratify patients into prognostic risk categories at the time of resection were identified. Results from two different cohorts lead to the identification of two microRNAs, miR-376a-3p and miR-888-5p, that were commonly downregulated in pLGGs with progression. MicroRNAs resulting from profiling were further validated by in-situ hybridization. Finally, enrichment analyses of these microRNAs were performed to elucidate their possible role in pLGG biology.

The fact that pLGG are a heterogeneous group of tumors and that each cohort has unique characteristics were reflected by the univariate analyses. Indeed, the use of two independent cohorts with diverse clinical features ascertained that the expression and/or variation of these microRNAs could not be attributed to specific features in both cohorts. PFS can account for miR-888-5p expression levels and the same cannot be excluded for miR-376a-3p. These results evidenced that both microRNAs of interest merited further investigation.

The ROC analysis confirmed their potential to act as prognostic biomarkers in pLGGs. In fact both microRNAs showed high specificity and sensitivity in distinguishing between the two subgroups of patients and their combination had an AUC of 0.8694 and a p-value of 0.0017.

MiR-376a-3p is a member of the microRNA cluster 379-656, consisting of 3 microRNAs (miR-376a-3p, miR-376b, miR-377-5p) mapped on chromosome 14 [100] and has already been described as a tumor suppressor microRNA in colorectal, prostate, melanoma and hepatocarcinoma [101-104], underlying that it could act as a pivotal player in cancer progression. MiR-376a-3p restoration in giant cell tumors of the bone stromal cells and osteosarcoma cells had the ability to significantly inhibit cell proliferation as well as migration and colony forming capacity [105-107]. Moreover, its restoration in-vivo in osteosarcoma xenografts reduced tumor uptake rates and tumor volumes, negatively influencing osteosarcoma cells aggressiveness [105]. The protein disulfide isomerase family A member 6 (PDIA6) is a validated miR-376a-3p target and is involved in promoting cancer resistance by inducing the shedding of the natural killer group 2, member D ligands and contributing to immune escape of the tumor [106]. Of note, the transcription factor and master cancer gene c-MYC is a validated miR-376a target gene [108]. Moreover, it is worth noting that in hepatocellular carcinoma cells the treatment with Tacrolimus and/or mTOR inhibitors induced a pro-apoptotic and anti-proliferative effect in a miR-376a-3p dependent fashion [109]. This observation supports the interesting role of miR-376a-3p in pLGG, where mTOR activation has been reported in the majority of these tumors [16,70] and Everolimus, an mTOR inhibitor, is underway to be used as frontline therapy in recurrent or progressive pLGG [110]. MiR-376a-3p has also been described as a possible predictive biomarker. Wen et al. identified a signature of four microRNAs, including miR-376a-3p, as a potential predictive marker of response to neoadjuvant chemoradiotherapy in esophageal squamous cell carcinoma [111]. Of note, miR-376a expression is reduced in adult glioma tissues and cells in respect to normal brain tissues and normal human astrocytes; its overexpression inhibited cancer cell growth and proliferation through the action of the validated target SP1, whose expression was related to glioma grade and overall survival of glioma patients [112]. Finally, miR-376a family members resulted under-expressed in sera from glioma patients compared to healthy controls, their low expression was associated with aggressive tumor progression and acted as independent factors of poor prognosis in glioma patients [112].

MiR-888-5p, is a member of a microRNA cluster consisting of 6 microRNAs (miR-888, miR-890, miR-891b, miR-892a, miR-892b, miR-892c) on chromosome X [100]. Deregulated expression of miR-888-5p has been reported in different solid tumors, such as hepatocellular carcinoma

[113,114], bladder cancer [115], prostate cancer [116-118], colorectal cancer [119,120], endometrial cancer [121], diffuse large B-cell lymphoma [122], breast cancer [123,124], glioblastoma [125] and lung adenocarcinoma [126,127].

MiR-888-5p has been described as both oncomiR and tumor suppressor, depending on the context. Indeed, miR-888-5p overexpression was reported to promote proliferation and metastatic potential of hepatocellular carcinoma cells by decreasing p53 expression [113] or by targeting SMAD4 [114]. MiR-888-5p overexpression and repression of SMAD4 was also observed in prostate cancer, along with RBL1 repression, promoting prostate cancer progression [117,118]. In addition, other targets of miR-888-5p were validated in prostate cancer, namely KLF5 and TIMP2 [116]. In colorectal cancer, miR-888-5p has been reported as a potent oncomiR and a prognostic factor for poor survival outcome [119,120]. In endometrial cancer high expression of miR-888-5p was associated with high-grade tumors, increased invasiveness and targeted progesterone receptor, a potent endometrial tumor suppressor [121]. Finally, in breast cancer miR-888-5p contributed to aggressiveness and metastasis by repression of adherens junction pathway and targeting of E-cadherin [124]. On the other hand, repression of miR-888-5p by the circular RNA circ-APC resulted in increased expression of APC and inhibited proliferation in diffuse large B-cell lymphoma tissues [122]. Interestingly, in invasive bladder cancer cells miR-888-5p hypomethylation and transactivation by E2F1 led to APLF repression. APLF is a chromatin modifier regulating c-NHEJ and the absence of miR-888-5p established an active E2F1/APLF/DCLRE1C axis particularly favorable for patient's survival. Similarly, the expression of miR-888 together with miR-892b and miR-892a was inversely correlated with MRI featuring an enhanced/necrosis ratio ≥ 1 in glioblastoma multiforme [125]. The role of miR-888-5p in lung adenocarcinoma appears context-dependent, indeed, its high expression was associated with clinical staging, while its expression was low in patients with recurrence when compared to patients without recurrence [126,127]. Notably, the studies where miR-888-5p has been associated with progression and investigated as a prognostic biomarker lend credence to the possibility that miR-888-5p can be used as a biomarker in pLGG.

Investigation of genes targeted by miR-376a-3p and miR-888-5p, followed by enrichment analysis, resulted in five genes reported in high-grade astrocytoma, grade 4 high-grade glioma, grade 4 malignant glioma and grade 4 astrocytoma (Table 7). Interestingly, four of these have been reported as mutated in a small percentage of grade 4 astrocytoma and up-regulated in different cancer types (DEFB132, ELOVL7, FGF12, ZNF714) [128-133], while high levels of IL15 were detected in the serum of glioblastoma patients [134]. The functional role of the aberrant

expression of these genes in cancer and specifically in high-grade gliomas could be mirrored in pLGG with progression by the loss of repression from the microRNAs of interest. A potential limit of the study is the number of analyzed samples, however the identification of two commonly dysregulated microRNAs in two independent cohorts with two different methods of detection corroborates the idea that these two microRNAs are valid candidates to be used as prognostic biomarkers already at the time of surgical resection. Since to date no other methods or biomarkers are available to distinguish partially resected pLGG that will experience progression from those that will remain stable, the discovery of trustable prognostic biomarkers could help clinicians choose the best treatment strategy. In conclusion, although further research is required to validate these results and shed light on the functional role of these microRNAs and their common target genes in pLGG, the analysis of miR-376a-3p and miR-888-5p may help guide the choice of a personalized therapy in pLGG after subtotal and/or partial surgical resection.

6. References

1. Packer RJ, Pfister S, Bouffet E, Avery R, Bandopadhayay P, Bornhorst M, Bowers DC, Ellison D, Fangusaro J, Foreman N (2016) Pediatric low-grade gliomas: implications of the biologic era. Neuro-oncology 19 (6):750-761

2. Louis DN, Perry A, Reifenberger G, Von Deimling A, Figarella-Branger D, Cavenee WK, Ohgaki H, Wiestler OD, Kleihues P, Ellison DW (2016) The 2016 World Health Organization classification of tumors of the central nervous system: a summary. Acta neuropathologica 131 (6):803-820

3. Pfister S, Witt O (2009) Pediatric Gliomas. In: von Deimling A (ed) Gliomas. Springer Berlin Heidelberg, Berlin, Heidelberg, pp 67-81. doi:10.1007/978-3-540-31206-2_4

4. Filbin MG, Sturm D Gliomas in children. In: Seminars in neurology, 2018. vol 01. Thieme Medical Publishers, pp 121-130

5. Yang RR, Aibaidula A, Wang W-w, Chan AK-Y, Shi Z-f, Zhang Z-y, Chan DTM, Poon WS, Liu X-z, Li W-c (2018) Pediatric low-grade gliomas can be molecularly stratified for risk. Acta neuropathologica 136 (4):641-655

6. Ryall S, Zapotocky M, Fukuoka K, Nobre L, Stucklin AG, Bennett J, Siddaway R, Li C, Pajovic S, Arnoldo A (2020) Integrated molecular and clinical analysis of 1,000 pediatric low-grade gliomas. Cancer Cell 37 (4):569-583. e565

7. Zhang J, Wu G, Miller CP, Tatevossian RG, Dalton JD, Tang B, Orisme W, Punchihewa C, Parker M, Qaddoumi I (2013) Whole-genome sequencing identifies genetic alterations in pediatric low-grade gliomas. Nature genetics 45 (6):602

8. Qaddoumi I, Orisme W, Wen J, Santiago T, Gupta K, Dalton JD, Tang B, Haupfear K, Punchihewa C, Easton J (2016) Genetic alterations in uncommon low-grade neuroepithelial tumors: BRAF, FGFR1, and MYB mutations occur at high frequency and align with morphology. Acta neuropathologica 131 (6):833-845

9. Sturm D, Pfister SM, Jones DT (2017) Pediatric gliomas: Current concepts on diagnosis, biology, and clinical management. Journal of Clinical Oncology:JCO. 2017.2073. 0242

10. Nicolaides TP, Li H, Solomon DA, Hariono S, Hashizume R, Barkovich K, Baker SJ, Paugh BS, Jones C, Forshew T (2011) Targeted therapy for BRAFV600E malignant astrocytoma. Clinical Cancer Research 17 (24):7595-7604

11. Schindler G, Capper D, Meyer J, Janzarik W, Omran H, Herold-Mende C, Schmieder K, Wesseling P, Mawrin C, Hasselblatt M (2011) Analysis of BRAF V600E mutation in 1,320 nervous system tumors reveals high mutation frequencies in pleomorphic xanthoastrocytoma, ganglioglioma and extra-cerebellar pilocytic astrocytoma. Acta neuropathologica 121 (3):397-405

12. Jones D, Kocialkowski S, Liu L, Pearson D, Ichimura K, Collins V (2009) Oncogenic RAF1 rearrangement and a novel BRAF mutation as alternatives to KIAA1549: BRAF fusion in activating the MAPK pathway in pilocytic astrocytoma. Oncogene 28 (20):2119

13. Jones DT, Kocialkowski S, Liu L, Pearson DM, Bäcklund LM, Ichimura K, Collins VP (2008) Tandem duplication producing a novel oncogenic BRAF fusion gene defines the majority of pilocytic astrocytomas. Cancer research 68 (21):8673-8677

14. Schubbert S, Shannon K, Bollag G (2007) Hyperactive Ras in developmental disorders and cancer. Nature Reviews Cancer 7 (4):295

15. Tatevossian RG, Lawson AR, Forshew T, Hindley GF, Ellison DW, Sheer D (2010) MAPK pathway activation and the origins of pediatric low-grade astrocytomas. Journal of cellular physiology 222 (3):509-514

16. Hütt-Cabezas M, Karajannis MA, Zagzag D, Shah S, Horkayne-Szakaly I, Rushing EJ, Cameron JD, Jain D, Eberhart CG, Raabe EH (2013) Activation of mTORC1/mTORC2 signaling in pediatric low-grade glioma and pilocytic astrocytoma reveals mTOR as a therapeutic target. Neuro-oncology 15 (12):1604-1614

17. Dienstmann R, Rodon J, Serra V, Tabernero J (2014) Picking the point of inhibition: a comparative review of PI3K/AKT/mTOR pathway inhibitors. Molecular cancer therapeutics 13 (5):1021-1031

18. Jacob K, Quang-Khuong D-A, Jones DT, Witt H, Lambert S, Albrecht S, Witt O, Vezina C, Shirinian M, Faury D (2011) Genetic aberrations leading to MAPK pathway activation mediate oncogene-induced senescence in sporadic pilocytic astrocytomas. Clinical Cancer Research 17 (14):4650-4660

19. Raabe EH, Lim KS, Kim JM, Meeker A, Mao X-g, Nikkhah G, Maciaczyk J, Kahlert U, Jain D, Bar E (2011) BRAF activation induces transformation and then senescence in human neural stem cells: a pilocytic astrocytoma model. Clinical Cancer Research 17 (11):3590-3599
20. Selt F, Hohloch J, Hielscher T, Sahm F, Capper D, Korshunov A, Usta D, Brabetz S, Ridinger J, Ecker J (2017) Establishment and application of a novel patient-derived KIAA1549: BRAF-driven pediatric pilocytic astrocytoma model for preclinical drug testing. Oncotarget 8 (7):11460
21. Mueller S, Phillips J, Onar-Thomas A, Romero E, Zheng S, Wiencke JK, McBride SM, Cowdrey C, Prados MD, Weiss WA (2012) PTEN promoter methylation and activation of the PI3K/Akt/mTOR pathway in pediatric gliomas and influence on clinical outcome. Neuro-oncology 14 (9):1146-1152
22. Ullrich NJ, Pomeroy SL, Kapur K, Manley PE, Goumnerova LC, Loddenkemper T (2015) Incidence, risk factors, and longitudinal outcome of seizures in long-term survivors of pediatric brain tumors. Epilepsia 56 (10):1599-1604
23. Gnekow AK, Kandels D, Van Tilburg C, Azizi AA, Opocher E, Stokland T, Driever PH, Van Meeteren AYS, Thomale UW, Schuhmann MU (2019) SIOP-E-BTG and GPOH Guidelines for Diagnosis and Treatment of Children and Adolescents with Low Grade Glioma. Klinische Pädiatrie 231 (03):107-135
24. Miklja Z, Pasternak A, Stallard S, Nicolaides T, Kline-Nunnally C, Cole B, Beroukhim R, Bandopadhayay P, Chi S, Ramkissoon SH (2019) Molecular profiling and targeted therapy in pediatric gliomas: review and consensus recommendations. Neuro-oncology 21 (8):968-980
25. Gajjar A, Bowers D, Karajannis M, Leary S, Witt H, Gottardo N (2015) Pediatric brain tumors: innovative genomic information is transforming the diagnostic and clinical landscape. Journal of Clinical Oncology:JCO-2014. doi:10.1200/JCO.2014.59.9217
26. Garcia MA, Solomon DA, Haas-Kogan DA (2016) Exploiting molecular biology for diagnosis and targeted management of pediatric low-grade gliomas. Future Oncology 12 (12):1493-1506
27. Gnekow AK, Walker DA, Kandels D, Picton S, Perilongo G, Grill J, Stokland T, Sandstrom PE, Warmuth-Metz M, Pietsch T (2017) A European randomised controlled trial of the addition of etoposide to standard vincristine and carboplatin induction as part of an 18-month treatment programme for childhood (≤ 16 years) low grade glioma–A final report. European Journal of Cancer 81:206-225
28. de Blank P, Bandopadhayay P, Haas-Kogan D, Fouladi M, Fangusaro J (2019) Management of pediatric low-grade glioma. Current opinion in pediatrics 31 (1):21-27
29. Sievert AJ, Lang S-S, Boucher KL, Madsen PJ, Slaunwhite E, Choudhari N, Kellet M, Storm PB, Resnick AC (2013) Paradoxical activation and RAF inhibitor resistance of BRAF protein kinase fusions characterizing pediatric astrocytomas. Proceedings of the National Academy of Sciences 110 (15):5957-5962
30. Greenberger BA, Pulsifer MB, Ebb DH, MacDonald SM, Jones RM, Butler WE, Huang MS, Marcus KJ, Oberg JA, Tarbell NJ (2014) Clinical outcomes and late endocrine, neurocognitive, and visual profiles of proton radiation for pediatric low-grade gliomas. International Journal of Radiation Oncology* Biology* Physics 89 (5):1060-1068
31. Jones DT, Banito A, Grünewald TG, Haber M, Jäger N, Kool M, Milde T, Molenaar JJ, Nabbi A, Pugh TJ (2019) Molecular characteristics and therapeutic vulnerabilities across paediatric solid tumours. Nature Reviews Cancer 19 (8):420-438
32. Jones DT, Hutter B, Jäger N, Korshunov A, Kool M, Warnatz H-J, Zichner T, Lambert SR, Ryzhova M, Quang DAK (2013) Recurrent somatic alterations of FGFR1 and NTRK2 in pilocytic astrocytoma. Nature genetics 45 (8):927
33. Rodriguez EF, Scheithauer BW, Giannini C, Rynearson A, Cen L, Hoesley B, Gilmer-Flynn H, Sarkaria JN, Jenkins S, Long J (2011) PI3K/AKT pathway alterations are associated with clinically aggressive and histologically anaplastic subsets of pilocytic astrocytoma. Acta neuropathologica 121 (3):407-420
34. Banerjee A, Jakacki RI, Onar-Thomas A, Wu S, Nicolaides T, Young Poussaint T, Fangusaro J, Phillips J, Perry A, Turner D (2017) A phase I trial of the MEK inhibitor selumetinib (AZD6244) in pediatric patients with recurrent or refractory low-grade glioma: a Pediatric Brain Tumor Consortium (PBTC) study. Neuro-oncology 19 (8):1135-1144

35. Jain P, Silva A, Han HJ, Lang S-S, Zhu Y, Boucher K, Smith TE, Vakil A, Diviney P, Choudhari N (2017) Overcoming resistance to single-agent therapy for oncogenic BRAF gene fusions via combinatorial targeting of MAPK and PI3K/mTOR signaling pathways. Oncotarget 8 (49):84697
36. Winter J, Jung S, Keller S, Gregory RI, Diederichs S (2009) Many roads to maturity: microRNA biogenesis pathways and their regulation. Nature cell biology 11 (3):228
37. Lin S, Gregory RI (2015) MicroRNA biogenesis pathways in cancer. Nature reviews cancer 15 (6):321-333. doi:10.1038/nrc3932
38. Lewis BP, Green RE, Brenner SE (2003) Evidence for the widespread coupling of alternative splicing and nonsense-mediated mRNA decay in humans. Proceedings of the National Academy of Sciences 100 (1):189-192
39. Calin GA, Dumitru CD, Shimizu M, Bichi R, Zupo S, Noch E, Aldler H, Rattan S, Keating M, Rai K (2002) Frequent deletions and down-regulation of micro-RNA genes miR15 and miR16 at 13q14 in chronic lymphocytic leukemia. Proceedings of the National Academy of Sciences 99 (24):15524-15529
40. Iorio MV, Ferracin M, Liu C-G, Veronese A, Spizzo R, Sabbioni S, Magri E, Pedriali M, Fabbri M, Campiglio M (2005) MicroRNA gene expression deregulation in human breast cancer. Cancer research 65 (16):7065-7070
41. Hasemeier B, Christgen M, Kreipe H, Lehmann U (2008) Reliable microRNA profiling in routinely processed formalin-fixed paraffin-embedded breast cancer specimens using fluorescence labelled bead technology. BMC biotechnology 8 (1):90
42. Nelson PT, Wang W-X, Wilfred BR, Tang G (2008) Technical variables in high-throughput miRNA expression profiling: much work remains to be done. Biochimica et Biophysica Acta (BBA)-Gene Regulatory Mechanisms 1779 (11):758-765
43. Cortez MA, Calin GA (2009) MicroRNA identification in plasma and serum: a new tool to diagnose and monitor diseases. Expert opinion on biological therapy 9 (6):703-711
44. Keller A, Leidinger P, Borries A, Wendschlag A, Wucherpfennig F, Scheffler M, Huwer H, Lenhof H-P, Meese E (2009) miRNAs in lung cancer-studying complex fingerprints in patient's blood cells by microarray experiments. BMC cancer 9 (1):353
45. Wang CT, Wang XZ, Tang YY, Zhang JC, Yu SL, Xu JZ, Bao ZM (2009) A rapid and cheap protocol for preparation of PCR templates in peanut. Electronic Journal of Biotechnology 12 (2):9-10
46. Creighton CJ, Reid JG, Gunaratne PH (2009) Expression profiling of microRNAs by deep sequencing. Briefings in bioinformatics 10 (5):490-497
47. McManus MT MicroRNAs and cancer. In: Seminars in cancer biology, 2003. vol 4. Elsevier, pp 253-258
48. Hayashita Y, Osada H, Tatematsu Y, Yamada H, Yanagisawa K, Tomida S, Yatabe Y, Kawahara K, Sekido Y, Takahashi T (2005) A polycistronic microRNA cluster, miR-17-92, is overexpressed in human lung cancers and enhances cell proliferation. Cancer research 65 (21):9628-9632
49. Bloomston M, Frankel WL, Petrocca F, Volinia S, Alder H, Hagan JP, Liu C-G, Bhatt D, Taccioli C, Croce CM (2007) MicroRNA expression patterns to differentiate pancreatic adenocarcinoma from normal pancreas and chronic pancreatitis. Jama 297 (17):1901-1908
50. Mattie MD, Benz CC, Bowers J, Sensinger K, Wong L, Scott GK, Fedele V, Ginzinger D, Getts R, Haqq C (2006) Optimized high-throughput microRNA expression profiling provides novel biomarker assessment of clinical prostate and breast cancer biopsies. Molecular cancer 5 (1):24
51. Chen C (2005) MicroRNAs as oncogenes and tumor suppressors. New England journal of medicine 353 (17):1768
52. Cao X, Yeo G, Muotri AR, Kuwabara T, Gage FH (2006) Noncoding RNAs in the mammalian central nervous system. Annu Rev Neurosci 29:77-103
53. Birks DK, Barton VN, Donson AM, Handler MH, Vibhakar R, Foreman NK (2011) Survey of MicroRNA expression in pediatric brain tumors. Pediatric blood & cancer 56 (2):211-216
54. Ho C-Y, Bar E, Giannini C, Marchionni L, Karajannis MA, Zagzag D, Gutmann DH, Eberhart CG, Rodriguez FJ (2012) MicroRNA profiling in pediatric pilocytic astrocytoma reveals biologically relevant targets, including PBX3, NFIB, and METAP2. Neuro-oncology 15 (1):69-82

55. Liu F, Xiong Y, Zhao Y, Tao L, Zhang Z, Zhang H, Liu Y, Feng G, Li B, He L (2013) Identification of aberrant microRNA expression pattern in pediatric gliomas by microarray. Diagnostic pathology 8 (1):158
56. Eguía-Aguilar P, Pérezpeña-Díazconti M, Benadón-Darszon E, de León FC-P, Gordillo-Domínguez L, Torres-García S, Sadowinski-Pine S, Arenas-Huertero F (2014) Reductions in the expression of miR-124-3p, miR-128-1, and miR-221-3p in pediatric astrocytomas are related to high-grade supratentorial, and recurrent tumors in Mexican children. Child's Nervous System 30 (7):1173-1181
57. Jones TA, Jeyapalan JN, Forshew T, Tatevossian RG, Lawson AR, Patel SN, Doctor GT, Mumin MA, Picker SR, Phipps KP (2015) Molecular analysis of pediatric brain tumors identifies microRNAs in pilocytic astrocytomas that target the MAPK and NF-κB pathways. Acta neuropathologica communications 3 (1):86
58. Braoudaki M, Lambrou G, Papadodima S, Stefanaki K, Prodromou N, Kanavakis E (2016) MicroRNA expression profiles in pediatric dysembryoplastic neuroepithelial tumors. Medical Oncology 33 (1):5
59. Laddha SV, Nayak S, Paul D, Reddy R, Sharma C, Jha P, Hariharan M, Agrawal A, Chowdhury S, Sarkar C (2013) Genome-wide analysis reveals downregulation of miR-379/miR-656 cluster in human cancers. Biology direct 8 (1):10
60. Skalsky RL, Cullen BR (2011) Reduced expression of brain-enriched microRNAs in glioblastomas permits targeted regulation of a cell death gene. PloS one 6 (9):e24248
61. Ames HM, Yuan M, Vizcaíno MA, Yu W, Rodriguez FJ (2017) MicroRNA profiling of low-grade glial and glioneuronal tumors shows an independent role for cluster 14q32. 31 member miR-487b. Modern Pathology 30 (2):204-216
62. Bongaarts A, Prabowo AS, Arena A, Anink JJ, Reinten RJ, Jansen FE, Spliet WG, Thom M, Coras R, Blümcke I (2018) MicroRNA519d and microRNA4758 can identify gangliogliomas from dysembryoplastic neuroepithelial tumours and astrocytomas. Oncotarget 9 (46):28103
63. Yuan M, Da Silva ACA, Arnold A, Okeke L, Ames H, Correa-Cerro LS, Vizcaino MA, Ho C-Y, Eberhart CG, Rodriguez FJ (2018) MicroRNA (miR) 125b regulates cell growth and invasion in pediatric low grade glioma. Scientific reports 8 (1):1-14
64. Júnior LGD, Lira RCP, Fedatto PF, Antonio DSM, Valera ET, Aguiar S, Yunes JA, Brandalise SR, Neder L, Saggioro FP (2019) MicroRNA profile of pediatric pilocytic astrocytomas identifies two tumor-specific signatures when compared to non-neoplastic white matter. Journal of neuro-oncology 141 (2):373-382
65. Nix JS, Yuan M, Imada EL, Ames H, Marchionni L, Gutmann DH, Rodriguez FJ (2020) Global microRNA profiling identified miR-10b-5p as a regulator of neurofibromatosis 1 (NF1)-glioma migration. Neuropathology and Applied Neurobiology
66. Bongaarts A, van Scheppingen J, Korotkov A, Mijnsbergen C, Anink JJ, Jansen FE, Spliet WG, den Dunnen WF, Gruber VE, Scholl T (2020) The coding and non-coding transcriptional landscape of subependymal giant cell astrocytomas. Brain 143 (1):131-149
67. Li Q, Shen K, Zhao Y, Ma C, Liu J, Ma J (2013) MiR-92b inhibitor promoted glioma cell apoptosis via targeting DKK3 and blocking the Wnt/beta-catenin signaling pathway. J Transl Med 11:32
. doi:10.1186/1479-5876-11-302
68. Sredni ST, Huang C-C, Suzuki M, Pundy T, Chou P, Tomita T (2016) Spontaneous involution of pediatric low-grade gliomas: high expression of cannabinoid receptor 1 (CNR1) at the time of diagnosis may indicate involvement of the endocannabinoid system. Child's Nervous System 32 (11):2061-2067
69. Tantawy M, Elzayat MG, Yehia D, Taha H (2018) Identification of microRNA signature in different pediatric brain tumors. Genetics and molecular biology 41 (1):27-34
70. Catanzaro G, Besharat ZM, Miele E, Chiacchiarini M, Po A, Carai A, Marras CE, Antonelli M, Badiali M, Raso A, Mascelli S, Schrimpf D, Stichel D, Tartaglia M, Capper D, von Deimling A, Giangaspero F, Mastronuzzi A, Locatelli F, Ferretti E (2018) The miR-139-5p regulates proliferation of supratentorial paediatric low-grade gliomas by targeting the PI3K/AKT/mTORC1 signalling. Neuropathology and Applied Neurobiology. doi:10.1111/nan.12479
71. Chiacchiarini M, Besharat ZM, Carai A, Miele E, Del Baldo G, Mastronuzzi A, Catanzaro G, Ferretti E (2020) Pediatric low-grade gliomas: molecular characterization of patient-derived cellular models. Child's Nervous System:1-8. doi:10.1007/s00381-020-04559-w

72. Po A, Silvano M, Miele E, Capalbo C, Eramo A, Salvat iV, Todaro M, Besharat ZM, Catanzaro G, Cucchi D, Coni S, Di Marcotullio L, Canettieri G, Vacca A, Stassi G, De Smaele E, Tartaglia M, Screpanti I, De Maria R, Ferretti E (2017) Noncanonical GLI1 signalling promotes stemness features and in-vivo growth in lung adenocarcinoma Oncogene. doi:10.1038/onc.2017.91
73. Tian Y, Rich BE, Vena N, Craig JM, MacConaill LE, Rajaram V, Goldman S, Taha H, Mahmoud M, Ozek M (2011) Detection of KIAA1549-BRAF fusion transcripts in formalin-fixed paraffin-embedded pediatric low-grade gliomas. The Journal of Molecular Diagnostics 13 (6):669-677
74. Diniz MG, Gomes CC, Guimarães BVA, Castro WH, Lacerda JCT, Cardoso SV, de Faria PR, Dias FL, Eisenberg ALA, Loyola AM (2015) Assessment of BRAFV600E and SMOF412E mutations in epithelial odontogenic tumours. Tumor Biology 36 (7):5649-5653
75. Hovestadt V, Jones DT, Picelli S, Wang W, Kool M, Northcott PA, Sultan M, Stachurski K, Ryzhova M, Warnatz H-J (2014) Decoding the regulatory landscape of medulloblastoma using DNA methylation sequencing. Nature 510 (7506):537-541
76. Miele E, Buttarelli F, Arcella A, Begalli F, Garg N, Silvano M, Po A, Baldi C, Carissimo G, Antonelli M, Spinelli G (2013) High-throughput microRNA profiling of pediatric high-grade gliomas. Neuro-oncology. doi:10.1093/neuonc/not215
77. Griffiths-Jones S, Saini HK, van Dongen S, Enright AJ (2007) miRBase: tools for microRNA genomics. Nucleic acids research 36 (suppl_1):D154-D158
78. Suzuki R, Shimodaira H (2006) Pvclust: an R package for assessing the uncertainty in hierarchical clustering. Bioinformatics 22 (12):1540-1542
79. Vlachos IS, Zagganas K, Paraskevopoulou MD, Georgakilas G, Karagkouni D, Vergoulis T, Dalamagas T, Hatzigeorgiou AG (2015) DIANA-miRPath v3. 0: deciphering microRNA function with experimental support. Nucleic acids research 43 (W1):W460-W466
80. Law AM, Yin JX, Castillo L, Young AI, Piggin C, Rogers S, Caldon CE, Burgess A, Millar EK, O'Toole SA (2017) Andy's Algorithms: new automated digital image analysis pipelines for FIJI. Scientific reports 7 (1):1-11. doi:10.1038/s41598-017-15885-6
81. Love MI, Huber W, Anders S (2014) Moderated estimation of fold change and dispersion for RNA-seq data with DESeq2. Genome biology 15 (12):550
82. Ater JL, Zhou T, Holmes E, Mazewski CM, Booth TN, Freyer DR, Lazarus KH, Packer RJ, Prados M, Sposto R (2012) Randomized study of two chemotherapy regimens for treatment of low-grade glioma in young children: a report from the Children's Oncology Group. Journal of clinical oncology 30 (21):2641
83. Wisoff JH, Sanford RA, Heier LA, Sposto R, Burger PC, Yates AJ, Holmes EJ, Kun LE (2011) Primary neurosurgery for pediatric low-grade gliomas: a prospective multi-institutional study from the Children's Oncology Group. Neurosurgery 68 (6):1548-1555
84. Fangusaro J, Bandopadhayay P (2020) The "Risk" in Pediatric Low-Grade Glioma. Cancer Cell 37 (4):424-425
85. Upadhyaya SA, Ghazwani Y, Wu S, Broniscer A, Boop FA, Gajjar A, Qaddoumi I (2017) Mortality in children with low-grade glioma or glioneuronal tumors: A single-institution study. Pediatric Blood & Cancer. doi:10.1002/pbc.26717
86. Peng Y, Croce CM (2016) The role of MicroRNAs in human cancer. Signal transduction and targeted therapy 1 (1):1-9
87. Rosenfeld N, Aharonov R, Meiri E, Rosenwald S, Spector Y, Zepeniuk M, Benjamin H, Shabes N, Tabak S, Levy A (2008) MicroRNAs accurately identify cancer tissue origin. Nature biotechnology 26 (4):462-469
88. Condrat CE, Thompson DC, Barbu MG, Bugnar OL, Boboc A, Cretoiu D, Suciu N, Cretoiu SM, Voinea SC (2020) miRNAs as biomarkers in disease: latest findings regarding their role in diagnosis and prognosis. Cells 9 (2):276
89. Baker SJ, Ellison DW, Gutmann DH (2016) Pediatric gliomas as neurodevelopmental disorders. Glia 64 (6):879-895
90. Khatua S, Wang J, Rajaram V (2015) Review of low-grade gliomas in children—evolving molecular era and therapeutic insights. Child's Nervous System 31 (5):643-652

91. Qiu G, Lin Y, Zhang H, Wu D (2015) miR-139-5p inhibits epithelial–mesenchymal transition, migration and invasion of hepatocellular carcinoma cells by targeting ZEB1 and ZEB2. Biochemical and biophysical research communications 463 (3):315-321
92. Krishnan K, Steptoe AL, Martin HC, Pattabiraman DR, Nones K, Waddell N, Mariasegaram M, Simpson PT, Lakhani SR, Vlassov A (2013) miR-139-5p is a regulator of metastatic pathways in breast cancer. Rna 19 (12):1767-1780
93. Zhang L, Dong Y, Zhu N, Tsoi H, Zhao Z, Wu CW, Wang K, Zheng S, Ng SS, Chan FK (2014) microRNA-139-5p exerts tumor suppressor function by targeting NOTCH1 in colorectal cancer. Molecular cancer 13 (1):124
94. Song M, Yin Y, Zhang J, Zhang B, Bian Z, Quan C, Zhou L, Hu Y, Wang Q, Ni S (2014) MiR-139-5p inhibits migration and invasion of colorectal cancer by downregulating AMFR and NOTCH1. Protein & cell 5 (11):851-861
95. Li RY, Chen LC, Zhang HY, Du WZ, Feng Y, Wang HB, Wen JQ, Liu X, Li XF, Sun Y (2013) MiR-139 inhibits Mcl-1 expression and potentiates TMZ-induced apoptosis in glioma. CNS neuroscience & therapeutics 19 (7):477-483
96. Dai S, Wang X, Li X, Cao Y (2015) MicroRNA-139-5p acts as a tumor suppressor by targeting ELTD1 and regulating cell cycle in glioblastoma multiforme. Biochemical and biophysical research communications 467 (2):204-210
97. Yue S, Wang L, Zhang H, Min Y, Lou Y, Sun H, Jiang Y, Zhang W, Liang A, Guo Y (2015) miR-139-5p suppresses cancer cell migration and invasion through targeting ZEB1 and ZEB2 in GBM. Tumor Biology 36 (9):6741-6749
98. He L, Thomson JM, Hemann MT, Hernando-Monge E, Mu D, Goodson S, Powers S, Cordon-Cardo C, Lowe SW, Hannon GJ (2005) A microRNA polycistron as a potential human oncogene. nature 435 (7043):828-833
99. Bergthold G, Bandopadhayay P, Bi WL, Ramkissoon L, Stiles C, Segal RA, Beroukhim R, Ligon KL, Grill J, Kieran MW (2014) Pediatric low-grade gliomas: how modern biology reshapes the clinical field. Biochimica et Biophysica Acta (BBA)-Reviews on Cancer 1845 (2):294-307
100. Kozomara A, Birgaoanu M, Griffiths-Jones S (2019) miRBase: from microRNA sequences to function. Nucleic acids research 47 (D1):D155-D162
101. Formosa A, Markert E, Lena A, Italiano D, Finazzi-Agro E, Levine A, Bernardini S, Garabadgiu A, Melino G, Candi E (2014) MicroRNAs, miR-154, miR-299-5p, miR-376a, miR-376c, miR-377, miR-381, miR-487b, miR-485-3p, miR-495 and miR-654-3p, mapped to the 14q32. 31 locus, regulate proliferation, apoptosis, migration and invasion in metastatic prostate cancer cells. Oncogene 33 (44):5173-5182
102. Wang Y, Jiang F, Xiong Y, Cheng X, Qiu Z, Song R (2020) LncRNA TTN-AS1 sponges miR-376a-3p to promote colorectal cancer progression via upregulating KLF15. Life sciences 244:116936
103. Zehavi L, Avraham R, Barzilai A, Bar-Ilan D, Navon R, Sidi Y, Avni D, Leibowitz-Amit R (2012) Silencing of a large microRNA cluster on human chromosome 14q32 in melanoma: biological effects of mir-376a and mir-376c on insulin growth factor 1 receptor. Molecular cancer 11 (1):44
104. Zheng Y, Yin L, Chen H, Yang S, Pan C, Lu S, Miao M, Jiao B (2012) miR-376a suppresses proliferation and induces apoptosis in hepatocellular carcinoma. FEBS letters 586 (16):2396-2403
105. Fellenberg J, Lehner B, Saehr H, Schenker A, Kunz P (2019) Tumor Suppressor Function of miR-127-3p and miR-376a-3p in Osteosarcoma Cells. Cancers 11 (12)
106. Fellenberg J, Sähr H, Kunz P, Zhao Z, Liu L, Tichy D, Herr I (2016) Restoration of miR-127-3p and miR-376a-3p counteracts the neoplastic phenotype of giant cell tumor of bone derived stromal cells by targeting COA1, GLE1 and PDIA6. Cancer letters 371 (1):134-141
107. Herr I, Sähr H, Zhao Z, Yin L, Omlor G, Lehner B, Fellenberg J (2017) MiR-127 and miR-376a act as tumor suppressors by in vivo targeting of COA1 and PDIA6 in giant cell tumor of bone. Cancer Letters 409:49-55
108. Wang Y, Cong W, Wu G, Ju X, Li Z, Duan X, Wang X, Gao H (2018) MiR-376a suppresses the proliferation and invasion of non-small-cell lung cancer by targeting c-Myc. Cell biology international 42 (1):25-33

109. Navarro Villarán E, Cruz Ojeda Pdl, Contreras L, González R, Negrete M, Rodríguez Hernández MA, Marín Gómez LM, Álamo Martínez JM, Calvo A, Gómez Bravo MÁ (2020) Molecular Pathways Leading to Induction of Cell Death and Anti-Proliferative Properties by Tacrolimus and mTOR Inhibitors in Liver Cancer Cells.
110. Kieran MW, Yao X, Macy M, Leary S, Cohen K, MacDonald T, Allen J, Boklan J, Smith A, Nazemi K (2014) Final results of a prospective multi-institutional phase II study of everolimus (rad001), an mtor inhibitor, in pediatric patients with recurrent or progressive low-grade glioma. A poetic consortium trial. Neuro-oncology 16 (suppl_3):iii27-iii27
111. Wen J, Luo K, Liu H, Liu S, Lin G, Hu Y, Zhang X, Wang G, Chen Y, Chen Z (2016) MiRNA expression analysis of pretreatment biopsies predicts the pathological response of esophageal squamous cell carcinomas to neoadjuvant chemoradiotherapy. Annals of surgery 263 (5):942-948
112. Li Y, Wu Y, Sun Z, Wang R, Ma D (2018) MicroRNA‐376a inhibits cell proliferation and invasion in glioblastoma multiforme by directly targeting specificity protein 1. Molecular medicine reports 17 (1):1583-1590
113. Hao E, Yu J, Xie S, Zhang W, Wang G (2017) Up-regulation of miR-888-5p in hepatocellular carcinoma cell lines and its effect on malignant characteristics of cells. Journal of Biological Regulators and Homeostatic Agents 31 (1):163-169
114. Li Y, Sun F, Ma X, Qu H, Yu Y (2019) MiR-888 promotes cell migration and invasion of hepatocellular carcinoma by targeting SMAD4. Eur Rev Med Pharmacol Sci 23 (5):2020-2027
115. Richter C, Marquardt S, Li F, Spitschak A, Murr N, Edelhäuser BA, Iliakis G, Pützer BM, Logotheti S (2019) Rewiring E2F1 with classical NHEJ via APLF suppression promotes bladder cancer invasiveness. Journal of Experimental & Clinical Cancer Research 38 (1):292
116. Hasegawa T, Glavich GJ, Pahuski M, Short A, Semmes OJ, Yang L, Galkin V, Drake R, Esquela-Kerscher A (2018) Characterization and evidence of the miR-888 cluster as a novel cancer network in prostate. Molecular Cancer Research 16 (4):669-681
117. Lewis H, Lance R, Troyer D, Beydoun H, Hadley M, Orians J, Benzine T, Madric K, Semmes OJ, Drake R (2014) miR-888 is an expressed prostatic secretions-derived microRNA that promotes prostate cell growth and migration. Cell cycle 13 (2):227-239
118. Valera VA, Parra-Medina R, Walter BA, Pinto P, Merino MJ (2020) microRNA Expression Profiling in Young Prostate Cancer Patients. Journal of Cancer 11 (14):4106
119. Bobowicz M, Skrzypski M, Czapiewski P, Marczyk M, Maciejewska A, Jankowski M, Szulgo-Paczkowska A, Zegarski W, Pawłowski R, Polańska J (2016) Prognostic value of 5-microRNA based signature in T2-T3N0 colon cancer. Clinical & experimental metastasis 33 (8):765-773
120. Gao SJ, Chen L, Lu W, Zhang L, Wang L, Zhu HH (2018) miR‐888 functions as an oncogene and predicts poor prognosis in colorectal cancer. Oncology Letters 15 (6):9101-9109
121. Hovey AM, Devor EJ, Breheny PJ, Mott SL, Dai D, Thiel KW, Leslie KK (2015) miR-888: a novel cancer-testis antigen that targets the progesterone receptor in endometrial cancer. Translational oncology 8 (2):85-96
122. Hu Y, Zhao Y, Shi C, Ren P, Wei B, Guo Y, Ma J (2019) A circular RNA from APC inhibits the proliferation of diffuse large B-cell lymphoma by inactivating Wnt/β-catenin signaling via interacting with TET1 and miR-888. Aging (Albany NY) 11 (19):8068
123. Huang S, Chen L (2014) MiR-888 regulates side population properties and cancer metastasis in breast cancer cells. Biochemical and biophysical research communications 450 (4):1234-1240
124. Huang S, Cai M, Zheng Y, Zhou L, Wang Q, Chen L (2014) miR-888 in MCF-7 side population sphere cells directly targets E-cadherin. Journal of Genetics and Genomics 41 (1):35-42
125. Li W, Chen H, Zhang W, Yan W, Shi R, Li S, Jiang T (2013) Relationship between magnetic resonance imaging features and miRNA gene expression in patients with glioblastoma multiforme. Chinese medical journal 126 (15):2881
126. Cao JX (2019) miR‐888 regulates cancer progression by targeting multiple targets in lung adenocarcinoma. Oncology reports 41 (6):3367-3376

127. Lu Y, Govindan R, Wang L, Liu P-y, Goodgame B, Wen W, Sezhiyan A, Pfeifer J, Li Y-f, Hua X (2012) MicroRNA profiling and prediction of recurrence/relapse-free survival in stage I lung cancer. Carcinogenesis 33 (5):1046-1054
128. Bhushan A, Singh A, Kapur S, Borthakar BB, Sharma J, Rai AK, Kataki AC, Saxena S (2017) Identification and Validation of Fibroblast Growth Factor 12 Gene as a Novel Potential Biomarker in Esophageal Cancer Using Cancer Genomic Datasets. OMICS: A Journal of Integrative Biology 21 (10):616-631
129. Consortium TITP-CAoWG (2020) Pan-cancer analysis of whole genomes. Nature 578 (7793):82
130. Institute WTS (2014) Catalogue of somatic mutations in cancer (COSMIC).
131. Machnik M, Cylwa R, Kiełczewski K, Biecek P, Liloglou T, Mackiewicz A, Oleksiewicz U (2019) The expression signature of cancer-associated KRAB-ZNF factors identified in TCGA pan-cancer transcriptomic data. Molecular oncology 13 (4):701-724
132. Patil V, Pal J, Somasundaram K (2015) Elucidating the cancer-specific genetic alteration spectrum of glioblastoma derived cell lines from whole exome and RNA sequencing. Oncotarget 6 (41):43452
133. Tamura K, Makino A, Hullin-Matsuda F, Kobayashi T, Furihata M, Chung S, Ashida S, Miki T, Fujioka T, Shuin T (2009) Novel lipogenic enzyme ELOVL7 is involved in prostate cancer growth through saturated long-chain fatty acid metabolism. Cancer research 69 (20):8133-8140
134. Nijaguna MB, Patil V, Urbach S, Shwetha SD, Sravani K, Hegde AS, Chandramouli BA, Arivazhagan A, Marin P, Santosh V (2015) Glioblastoma-derived macrophage colony-stimulating factor (MCSF) induces microglial release of insulin-like growth factor-binding protein 1 (IGFBP1) to promote angiogenesis. Journal of Biological Chemistry 290 (38):23401-23415